How are nitrogen availability, fine-root mass, and nitrogen uptake related empirically?

Implications for models and theory

Running Head: N uptake, N availability, and fine-root mass

Authors: Ray Dybzinski[1]*, Angelo Kelvakis[1], John McCabe[1], Samantha Panock[1], Kanyarak Anuchitlertchon[1], Leah Vasarhelyi[1], M. Luke McCormack[2], Gordon G. McNickle[3,4], Hendrik Poorter[5,6], Clare Trinder[7], and Caroline E. Farrior[8]

[1]Institute of Environmental Sustainability, Loyola University Chicago, Chicago, Illinois 60660 USA

[2] Department of Plant and Microbial Biology, 140 Gortner Laboratory, 1479 Gortner Avenue, University of Minnesota, St Paul, MN 55108, USA

[3] Department of Botany and Plant Pathology, Purdue University, 915 W State St., West Lafayette, IN, 47907

[4] Purdue Center for Plant Biology, Purdue University, West Lafayette, IN, 47907

[5]Plant Sciences (IBG2), Forschungszentrum Jülich GmbH, D-52425 Jülich, Germany

[6]Department of Biological Sciences, Macquarie University, North Ryde, NSW 2109, Australia

[7]School of Biological Sciences, Cruickshank Building, University of Aberdeen, Aberdeen, AB24 3UL, UK

[8]Department of Integrative Biology, University of Texas at Austin, 2415 Speedway, Austin, Texas 78712

***corresponding author**; phone: 1-773-760-4092; fax: 1-773-508-8924; postal: 312 BVM Hall, Loyola University Chicago, Chicago, IL 60660; email: rdybzinski@LUC.edu

Keywords: competition, dynamic global vegetation model (DGVM), fine roots, game theory, nitrogen (N), over-proliferation, terrestrial biosphere model (TBM)

Type: Primary Research Article

Word counts: 6319 (introduction through acknowledgements), 263 (abstract)

References: 65; **Text Boxes:** 0; **Tables:** 1 table; **Figures:** 7 figures, all color; **Supporting information:** detailed SOM materials & methods, 18 additional color figures, and 4 tables

Abstract

Understanding the effects of global change in terrestrial communities requires an understanding of how limiting resources interact with plant traits to affect productivity. Here, we focus on nitrogen and ask whether plant community nitrogen uptake rate is determined (i) by nitrogen availability alone or (ii) by the product of nitrogen availability and fine-root mass. Surprisingly, this is not empirically resolved. We performed controlled microcosm experiments and reanalyzed published pot experiments and field data to determine the relationship between community-level nitrogen uptake rate, nitrogen availability, and fine-root mass for 46 unique combinations of species, nitrogen levels, and growing conditions. We found that plant community nitrogen uptake rate was unaffected by fine-root mass in 63% of cases and saturated with fine-root mass in 29% of cases (92% in total). In contrast, plant community nitrogen uptake rate was clearly affected by nitrogen availability. The results support the idea that although plants may over-proliferate fine roots for individual-level competition, it comes without an increase in community-level nitrogen uptake. The results have implications for the mechanisms included in coupled carbon-nitrogen terrestrial biosphere models (CN-TBMs) and are consistent with CN-TBMs that operate above the individual scale and *omit* fine-root mass in equations of nitrogen uptake rate but inconsistent with the majority of CN-TBMs, which operate above the individual scale and *include* fine-root mass in equations of nitrogen uptake rate. For the much smaller number of CN-TBMs that explicitly model individual-based belowground competition for nitrogen, the results suggest that the relative (not absolute) fine-root mass of competing individuals should be included in the equations that determine individual-level nitrogen uptake rates. By providing empirical data to support the assumptions used in CN-TBMs, we put their global climate change predictions on firmer ground.

Introduction

Increasing the mechanistic detail of the terrestrial biosphere models (TBMs) used to predict global climate change requires functional relationships between plant-, community-, and ecosystem-level processes (Lichstein *et al.*, 2014, Fisher *et al.*, 2015, Weng *et al.*, 2015, Fisher *et al.*, 2018). However, empirically-based information about these relationships is often lacking. Empirical data may fail to provide guidance either because sufficient data do not exist or because data are contingent on variables that do not appear in the TBM. Thus, targeted empirical studies that use model-relevant variables are important for increasing the accuracy of model predictions.

Among the recent advances in TBMs is the coupling of carbon dynamics with nitrogen dynamics (Hungate *et al.*, 2003, Wang & Houlton, 2009, Peñuelas *et al.*, 2013), which was spurred by the recognition that many or most terrestrial ecosystems are (at least) co-limited by nitrogen availability (LeBauer & Treseder, 2008). Operationally, this coupling requires interaction between the carbon and nitrogen statuses of plants and soils (Thornton *et al.*, 2007, Zaehle *et al.*, 2010, Gerber *et al.*, 2013). One of the important mechanisms of interaction is the process of plant community nitrogen uptake rate (Warren *et al.*, 2015). From our survey of twelve coupled carbon-nitrogen TBMs (CN-TBMs, summarized in Table S1), one third of CN-TBMs assume that nitrogen uptake rate is driven only by nitrogen availability (Fig. 1a) whereas two-thirds of CN-TBMs assume that nitrogen uptake rate is some function that depends on both nitrogen availability and fine-root mass (Fig. 1b,c). Most CN-TBMs include a variety of other dependencies, including temperature and plant demand. Although there are exceptions, the models that include fine-root dependence are more recent (Table S1). This is because fine roots take up nitrogen, and so adding fine roots to the nitrogen uptake function seems like an obvious mechanistic improvement (e.g. Ghimire *et al.*, 2016).

It may seem evident that models that include fine-root mass in their nitrogen uptake rate functions should better approximate reality. *A plant community with zero fine-root mass will take up zero nitrogen, and the uptake rate must increase with root mass from that obvious starting point.* Moreover, there exists

a wealth of physiological theory and data on fine-root function that is normalized on a per-fine-root mass basis (Kronzucker *et al.*, 1995, Bassirirad, 2000, Tinker & Nye, 2000), such as the Michaelis-Menten uptake kinetics for nitrate and ammonium. However, per-fine-root mass based traits may not scale linearly to the stand-level at which CN-TBMs are parameterized for several reasons, including soil resource and fine-root heterogeneity, interactions with other limiting resources, and game-theoretic fine-root "over-proliferation."

Fine-root over-proliferation is perhaps easiest to understand as a belowground analog to the evolution of height in trees (Givnish, 1982, Falster & Westoby, 2003). Trees evolved height not because it is optimal for light capture; trees in a tall forest receive no more light than a shrub in a nearby clearing. Instead, it was the fitness benefit that individuals received by being *relatively* taller than their neighbors that allowed them to more than replace themselves in subsequent generations and for directional selection to thus increase average height allocation. As absolute tree height increased, a fitness benefit kept going to individuals that were *relatively* taller, which continued to drive selection to greater height allocation. Similarly, individuals with *relatively* greater fine-root mass (or area) than their neighbors experienced greater nitrogen uptake rates via mass flow and diffusion. If nitrogen was limiting, this conferred a fitness benefit that allowed them to more than replace themselves in subsequent generations and for directional selection to thus increase average fine-root mass. As absolute fine-root mass increased, a fitness benefit kept going to individuals that had *relatively* greater fine-root mass, which continued to drive selection to greater fine-root mass (Gersani *et al.*, 2001, Craine, 2006, McNickle & Dybzinski, 2013).

Like tree height, fine-root over-proliferation is driven by individual-level selection but has consequences at the community-level. To the extent that fine-root over-proliferation has occurred, it may actually decouple *community-level* fine-root mass from *community-level* nitrogen uptake rates (Dybzinski *et al.*, 2011, Dybzinski *et al.*, 2015). To use an analogy, extant fine-root systems *at the community-level* may be like a huge sponge that is brought to soak up a small spill, i.e. the community has "surplus" uptake capacity due to its evolutionary history. If fine-root over-proliferation is an important factor in

plant systems, then the CN-TBMs that *do not* make nitrogen uptake rates a function of fine-root mass (Fig. 1a) may be closer to reality than the other, generally newer ones that do (Fig. 1b,c). This clearly calls for an empirical resolution.

Here, we repurpose a classic experimental method (van der Werf *et al.*, 1993) to elucidate the relationship between plant community nitrogen uptake rate, community fine-root mass, and nitrogen availability (Fig. 2). Briefly, via sequential harvest of numerous plants growing from seed in microcosms we track (1) total plant nitrogen over time and (2) total fine-root mass over time. As long as plant nitrogen losses are negligible for the seedlings, the derivative of total plant nitrogen with respect to time is necessarily the nitrogen uptake rate (Garnier, 1991). We relate this nitrogen uptake rate to fine-root mass at any given time point to determine the functional relationship between plant community nitrogen uptake rate and fine-root mass. We determine the dependence on nitrogen availability by growing sets of plants with different soil nitrogen availabilities. Importantly, the method requires no assumptions about root physiology or root over-proliferation. We used this methodology with microcosms of three species in semi-hydroponic sand culture, with microcosms of 14 species in soil, and with microcosms of a two-species replacement series in sand culture. We also include reanalyzed data from two other published pot experiments for which the data outlined above were available and from seven forest field studies for which fine-root mass and community-level plant nitrogen uptake rates were measured. In total, we present results from 46 unique species, nitrogen levels, and growing conditions.

Material and Methods

Overview

We present methods and results from five separate activities in the main text: (1) a sand culture microcosm experiment, (2) a soil culture microcosm experiment, (3) a sand culture two-species replacement series microcosm experiment, (4) previously-published pot experiments reanalyzed, and (5) previously-published field data reanalyzed. Of the three experiments that we conducted (1-3), the main

differences were substrate (sand versus soil), the origin of plant-available nitrogen (liquid fertilizer for sand versus natural soil organic matter decomposition and nitrogen mineralization for soil), and the numbers and identities of the species used (1: three species, 2: fourteen species, and 3: two species). We first describe how the data were collected for each of these activities and then follow it with a description of the methods of analysis, which are largely shared by the different activities.

Note that the supplemental online material (SOM) also includes details and results of a separate microcosm experiment that used the same methods but that additionally manipulated the density of seedlings per microcosm.

Data collection: (1) Sand culture microcosm experiment

Experiment 1 was conducted with microcosms of plants grown in sand in pots between September and December of 2016 in the greenhouse facility in the Institute of Environmental Sustainability, Loyola University Chicago, Chicago, Illinois, USA. Average low and high temperatures were 19 °C and 28 °C. We supplemented ambient sunlight with LumiGrow Pro 325 LED lights (Emeryville, California, USA) for 14 hours a day, and the average daily light integral over the duration of the experiment was 6.7 mol photons m^{-2} d^{-1}. We used *Pinus sylvestris*, a coniferous tree, *Schizachyrium scoparium*, a C4 grass, and *Poa pratensis*, a C3 grass (Sheffield's Seed Company, Locke, New York, USA) growing in a 1:1 mix (volume basis) of washed silica sand and calcified clay. So that we knew exactly how much nitrogen was available to the plants (e.g. Fig. S5), we used 0.35 L ribbed polystyrene "party cups" with no drainage, which guaranteed that no supplied nitrogen would be leached out.

We treated each species with three different nitrogen application rates, with two replicates per nitrogen application rate per each of eleven weekly harvests. This therefore is a regression experiment where low replication for a single harvest is counterbalanced by a large number of harvests (Hughes & Freeman, 1967, Cottingham *et al.*, 2005). In all, each species had 3 nitrogen levels, 11 harvests, and 2 replicates for 66 microcosms per species and 198 microcosms total. We seeded each microcosm with

approximately 12 seeds, which we gently misted for two weeks before initiating the regular fertigation and watering protocol described below. The germination rates of *Pinus* and *Poa* (median = 9/microcosm for each) were much higher than the germination rate of *Schizachyrium* (median = 3/microcosm, Fig. S1). Within each species, we conducted a two-way ANOVA of harvest date and nitrogen treatment on the number of seedlings per microcosm and found no significant effects and no trends, indicating that the variation in seedling numbers (Fig. S1) was not significantly different between experimental treatments nor confounded with them.

We prepared liquid fertilizer by combining 1.34 g L^{-1} minimal-nitrogen Hoagland's solution ("Hoagland's No. 2 Basal Salt Mixture without nitrogen," Caisson Laboratories, Smithfield, Utah, USA) with 0.02, 0.10, or 0.5 g L^{-1} ammonium nitrate (NH_4NO_3) to create an exponential gradient of 0.25, 1.25, and 6.25mM nitrogen solutions with a constant background of all other essential macro- and micro-nutrients. These translate to application rates of 0.057, 0.237, and 1.139 mg N d^{-1}. Based on the best methodology determined by pilot experiments, we fertigated on Mondays, Wednesdays, and Fridays with 15 ml per microcosm of the solutions described above. In order to minimize water limitation across the experiment, we watered all microcosms with 5, 10, or 15 ml deionized water as needed on the days we did not fertigate (later in the experiment we occasionally gave additional water to high-biomass/high-transpiration microcosms so that their substrate moisture was comparable to other microcosms). The first and last harvests occurred 25 and 95 days after seeding.

Data collection: (2) Soil microcosm experiment

We conducted experiment 2 between March and July of 2017 using the same facilities and lighting described above for experiment 1. Average low and high temperatures were 20 °C and 30 °C, and the average daily light integral over the duration of the experiment was 10.9 mol m^{-2} d^{-1}. We used four angiosperm tree species: *Betula papyrifera, Acer rubrum, Liquidambar styraciflua* (the species used in the ORNL FACE study, Norby *et al.*, 2005), and *Robinia pseudoacacia*; an herbaceous angiosperm:

Trifolium pretense (not inoculated with rhizobium and no N_2-fixing nodules observed at harvest); the C_4 & C_3 grasses used in the sand culture experiment: *Schizachyrium scoparium* and *Poa pratensis*; and seven gymnosperm tree species: *Picea abies*, *Picea glauca*, *Pinus taeda* (the species used in the Duke FACE study, Norby *et al.*, 2005), *Pinus banksiana*, *Pinus resinosa*, *Pinus strobus*, and *Pinus sylvestris* (which was also used in our sand culture experiment). We used an exponentially increasing soil fertility gradient by combining soil (SunGro Propagation Mix, Agawam, Massachusetts, USA) with a sand/turface mix in the following ratios by volume: 4:96, 20:80, and 100:0. Throughout the experiment, we added no nitrogen to the substrate; all plant-available nitrogen was mineralized from organic nitrogen in the soil. We used 0.44 L cubic pots that, unlike our sand-culture experiments, had free drainage. We allowed free drainage for two reasons. First, open pots were easier to maintain than closed pots. Second, because we did not have precise information on nitrogen mineralization in the soil, we could not accurately calculate the fraction of the supply that was taken up anyway, removing the only reason to use a closed pot. We watered the microcosms uniformly as needed, typically every other day.

Because we were interested in distributing our sampling effort of 504 microcosms across as many species as possible, we used one replicate per species per fertility level per each of 12 weekly harvests, again following a regression approach where low replication for a single harvest is balanced by frequent harvests (Hughes & Freeman, 1967, Cottingham *et al.*, 2005). In all, each species had 3 fertility levels, 12 harvests, and 1 replicate for 36 microcosms per species and 504 microcosms total. We planted approximately 10 seeds per species and then thinned to near constant density per species (Fig. S7). Three species failed to establish in the lower fertility soils (*Betula*, *Robinia*, and *Trifolium*). The median number of seeds per microcosm were: *Betula* 3, *Acer* 1, *Liquidambar* 4, *Robinia* 4, *Trifolium* 5.5, *Schizachyrium* 3, *Poa* 5, *Picea abies* 3, *P. glauca* 2, *Pinus taeda* 3, *P. banksiana* 4, *P. resinosa* 3, *P. strobus* 3, and *P. sylvestris* 4. The first and last harvests occurred approximately 19 and 110 days after seeding (some species were offset by a week or two because of slow germination).

Consistent with visual impressions of their growth, we separately analyzed leaf mass, stem + taproot mass, fine-root mass, total plant mass, and total plant nitrogen and found only modest differences between the 20:80 and 4:96 fertility treatments (Table S3). We thus merged data from these two treatments into a single "low fertility" treatment with greater replication.

Data collection: (3) Sand culture two-species replacement series microcosm experiment

We conducted experiment 3 between March and July of 2017 using the same facilities and lighting described above for experiment 1, except that we used only the intermediate 0.10 g L^{-1} (1.25 mM) ammonium nitrate (NH_4NO_3) treatment.

The goal of this experiment was to determine if an individual plant's *fraction* of community-level nitrogen uptake, $U_i/\sum U$, correlates with its *fraction* of community-level fine-root mass, $R_i/\sum R$, i.e. is relative fine-root mass related to competitive ability for limiting nitrogen, $R_i/\sum R \propto U_i/\sum U$? We were interested in *individual*-level competition, not *species*-level competition. We grew two species from the sand culture microcosm experiment together, *Schizachyrium* and *Poa*, not because we were interested in species-level competition, but rather because we believed we could separate *Schizachyrium* and *Poa* fine roots by appearance. Thus, the experiment really determines if a population's (e.g. *Schizachyrium's*) *fraction* of the total fine-root mass correlates with its *fraction* of the total nitrogen taken up by the community. This is a reasonable proxy for individual-level insights because if $R_i/\sum R \propto U_i/\sum U$ is true then $nR_i/\sum R \propto nU_i/\sum U$ must also be true, where n is the number of individuals in the *Schizachyrium* population.

To examine the anticipated effects of density and frequency dependence, we thinned microcosms to four unique density and frequency combinations: one *Schizachyrium* + two *Poa* individuals, three *Schizachyrium* + six *Poa* individuals, two *Schizachyrium* + one *Poa* individual, and six *Schizachyrium* + three *Poa* individuals. We created 12 replicates of each combination (4 combinations x 12 replicates = 48 microcosms total), which we harvested weekly once the seedlings were established (i.e. 12 harvests total).

For the first four harvests, we were completely confident in our separation of *Schizachyrium* and *Poa* fine roots because the root systems of individual plants could be separated without tearing. We were moderately confident in our ability to separate the species for harvests five through eight; deeper fine roots sometimes tore and it was not always obvious which species they belonged to. We were not very confident in our ability to separate the species for the last four harvests, where a great deal of tearing occurred. We present relative uptake data for only the first four harvests and community-level measures across all the harvests. However, the relative uptake trends observed in the eight harvests for which we are not perfectly confident about species separation are similar to those in the first four harvests (Fig. S15). Aboveground mass was always separated to species with confidence.

Data collection: (4) Previously-published pot experiments, reanalyzed

Poorter *et al.* (1995) grew an inherently fast-growing C3 grass, *Holcus lanatus*, and an inherently slow-growing C3 grass, *Deschampsia flexuosa* in semi-hydroponic sand culture using two different levels of nitrogen fertigation in a growth chamber. Their experiment lasted for between 21 days and 49 days from first harvest, depending on growth rate, with harvests thrice weekly and between six and eight replicates per unique treatment per harvest.

Trinder *et al.* (2012) grew the C3 grass *Dactylis glomerata* and the forb *Plantago lanceolata* in an agricultural soil. Their experiment lasted 76 days, with 17 harvests of three replicates per harvest. Unlike our microcosm experiments, both of these studies used just one seedling per pot (hence our decision to refer to them as "pot experiments" and not "microcosm experiments"). Further details can be found in the original publications.

Data collection: (5) Previously-published field data reanalyzed

Because many of the special conditions of microcosm-grown plants (e.g. soil volume, environmental conditions, ontogeny, community composition) may limit the generalizability of our

experiments (Poorter *et al.*, 2016), we also sought data from field studies that would allow us to relate plant nitrogen uptake rate with fine-root mass. We searched the following string without the outermost quotes "("nitrogen uptake" or "N uptake") and ("fine root" or "fine roots")" in Web of Science (webofknowledge.com) on 26 July 2017, which returned 178 results. We went through the results and found seven field studies that reported per unit soil area plant community nitrogen uptake rates and fine-root mass for multiple plots within the same geographic area. We contacted authors of studies that appeared to collect, but not report, these data. "Alaska taiga" sampled stands along an elevational gradient in low fertility soil at the Bonanza Creek Experimental Forest (Ruess *et al.*, 1996). "Aspen FACE" used newly-planted temperate *Populus*, *Acer*, and *Betula* tree saplings in intermediate fertility soil under ambient or elevated CO_2 (Finzi *et al.*, 2007). "Wisconsin temperate" used ~50 year old monotypic forest plantations of different species in intermediate fertility soil at the University of Wisconsin arboretum (Nadelhoffer *et al.*, 1985). "Duke FACE" used an ~18 year old *Pinus taeda* plantation in low fertility soil under ambient or elevated CO_2 (Finzi *et al.*, 2007). "Pop-Euro FACE" used a *Populus* sapling plantation in high fertility soil under ambient or elevated CO_2 (Finzi *et al.*, 2007). "Japan deciduous" used ~100 year old cool-temperate deciduous forests with topographical changes in soil nitrogen (Tateno *et al.*, 2004, Tateno & Takeda, 2010). Finally, "ORNL FACE" used a ~14 year old *Liquidambar styraciflua* plantation in intermediate fertility soil under ambient or elevated CO_2 (Finzi *et al.*, 2007). Where multiple years of data existed, we averaged by experimental unit to avoid pseudo-replication. We present details on each study's methods for calculating nitrogen uptake rate and fine-root mass in Table S4.

Analysis: Harvests & calculations for microcosm and pot experiments 1 – 4

In all of the microcosm (1-3) and pot experiments (4), plants were harvested at regular intervals. At each harvest, biomass was separated into leaf, stem (including thick tap roots where present), and fine roots. Except for thick tap roots, all roots were less than 1 mm diameter and thus classified as "fine roots", and no necrotic roots were observed at harvest (including the previously-published studies). Unlike field

studies, where it is challenging to estimate fine-root mass, we were able to wash substrate clear of fine roots and confidently collect all of the fine-root mass in a microcosm, i.e. we did not subsample.

After drying, weighing, and grinding, tissue nitrogen concentrations were measured via combustion or, for Poorter et al. (1995), the Kjeldahl method. The previously published studies used slightly different methods of estimating tissue nitrogen concentrations. Poorter *et al.* (1995) determined tissue nitrogen concentrations using the combined plant material from all harvests (i.e. spanning all the replicates across the entire duration of the experiment), but separately for each organ, species, and nitrogen level. Trinder *et al.* (2012) determined tissue nitrogen concentrations using each replicate by itself, but with all organs combined. In experiments 1-3, we determined tissue nitrogen concentrations separately for leaf, stem (when applicable), and fine roots for each replicate. Because it is difficult to precisely measure nitrogen concentrations using the small mass typical of seedlings, we performed a data averaging procedure in the spirit of the averaging used by Poorter *et al.* (1995) but which does not obscure possible changes in tissue nitrogen concentrations with ontogeny: we fit splines to our nitrogen concentration data by harvest date for every unique treatment and organ, omitted outliers (identified as having residuals above or below the predicted value by 1.5 standard deviations), fit a new spline to the remaining data (i.e. the splines in Figs. S3a-f, S9, and S13), and used the predicted value at a given harvest date when calculating total plant nitrogen. We used a cubic smoothing spline (specifically, the R function *smooth.spline* with df=3 (R Core Team, 2015), R version 3.2). Of the 105 fit splines of nitrogen concentration versus time (Figs. S3, S9, S13, Table S5), the goodness of fit (R^2) ranged from 0.09 to 0.98, with a median of 0.56 and a mean of 0.57.

For all microcosm (1-3) and pot experiments (4), total plant nitrogen content was calculated using the tissue nitrogen concentrations described above and replicate-level dry biomass values, summed across organs as appropriate. For our microcosm experiments 1-3, we subtracted the small amount of the nitrogen contained in seeds (Table S2) from total plant nitrogen to ensure that our final values reflected plant nitrogen uptake rate, rather than utilization of nitrogen provisioned within the seed. The impact of

this correction is slight. We extrapolated tissue mass per microcosm or pot to standard area-based measures by dividing by microcosm or pot surface area.

To estimate the instantaneous plant community nitrogen uptake *rate* (i.e. a flux), we calculated the derivative of a spline fit of total plant nitrogen (a pool) versus time at harvest (Figs. 2a, S4, S10, S14, S16a-d). We used a cubic smoothing spline (specifically, the R functions *smooth.spline* and *predict* (R Core Team, 2015), R version 3.2), to numerically calculate this derivative, allowing for the possibility that plants might switch their uptake rates to different functional forms of dependence on nitrogen availability or fine-root mass during the experiment. Of the 52 fit splines of total plant nitrogen versus time at harvest (Table S5), the goodness of fit (R^2) ranged from 0.45 to 1.00, with a median of 0.85 and a mean of 0.80. We paired those derivatives with predicted fine-root mass at each harvest (Figs. 2b, S2, S8, S12, S16) to determine the relationship between fine-root mass and nitrogen uptake rate (Fig. 2c). By repeating this for different species and nitrogen treatments, we were able to determine – for the first time – the full relationship between nitrogen availability, fine-root mass, and nitrogen uptake rate. The method is similar to the method used by van der Werf *et al.* (1993), except that we do not divide the nitrogen uptake rate by total fine-root mass before reporting results. We bootstrapped this process by randomly sampling with replacement the same number of fine-root mass and total plant nitrogen data points from the relevant data set (i.e. experiment, species, nitrogen level) and then recalculating the plant nitrogen uptake rate from the bootstrapped data. We repeated this process 500 times per experiment, species, and nitrogen level in order to provide an estimate of uncertainty.

Analysis: Model selection for all activities, 1 – 5

For every unique relationship between plant community nitrogen uptake rate (*NUR*) and fine-root mass (*F*), we used maximum likelihood methods to fit parameters (*c*, *m*, *v*, *k*), along with the standard deviation of residual data, for each of the three relationships used by CN-TBMs and shown in Fig. 1: mean (i.e. linear with zero slope), $NUR = c$; linear with zero intercept, $NUR = mF$; and saturating with

zero intercept, $NUR = \frac{vF}{k+F}$. We used the Nelder-Mead method of maximum likelihood estimation to estimate parameter values (Fig. 2d), by applying the *mle2* function in the bbmle package for R (Bolker & R Core Team, 2017). Given the log-likelihood values and parameter numbers for each model (noting that, in addition to *c*, *m*, *v*, or *k*, each model needed the additional parameter of the standard deviation of residual data) we calculated each model's AICc score (Cavanaugh, 1997) and ranked them from lowest (most parsimonious) to highest (least parsimonious) (Fig. 2e). In the rare instances when the difference between the lowest and second-lowest AICc scores was less than or equal to two, we deemed both models equally parsimonious.

Results

Across all 46 unique species, nitrogen levels, and growing conditions examined, plant community nitrogen uptake rate was independent of fine-root mass in 31 (63%), linearly related to fine-root mass in 4 (8%), and saturated with fine-root mass in 14 (29%) (Table 1, note that three cases were equally-well explained by independent and saturating fits).

Microcosm and pot experiments 1 – 4

In the microcosm (exps. 1 – 3) and pot experiments (exp. 4), both biomass (Figs. S2, S8, S12, S16) and total plant nitrogen (Figs. S4, S10, S14) generally increased at a greater rate at higher nitrogen availability, and root mass fraction generally decreased with increasing nitrogen availability (Figs. S2, S8, S12, S16). Tissue nitrogen concentrations generally decreased over time (Figs. S3, S9, S13). For the sand culture experiment (exp. 1), the fraction of supplied nitrogen taken up by plants increased with time (Fig. S5). Overall, different species exhibited qualitatively similar but quantitatively different responses for all of these measures.

For the sand culture microcosm experiment (exp. 1), plant community nitrogen uptake rates were independent of fine-root mass but increased with nitrogen availability across all three species (Fig. 3). For

the soil microcosm experiment (exp. 2), plant community nitrogen uptake rates were independent of fine-root mass in 15 cases, linearly-related to fine-root mass in two cases, and saturated at low fine-root mass in nine cases (Fig. 4). There were no obvious trends in the distribution of these responses across angiosperms versus gymnosperms or between low and high nitrogen availability. As in the sand culture experiment (exp. 1), plant community nitrogen uptake rates in the soil experiment (exp. 2) increased with nitrogen availability (Fig. 4). For the sand culture two-species replacement series microcosm experiment (exp. 3), the fraction of nitrogen taken up by *Schizachyrium* was positively correlated with its fine-root mass (Figs. 5a, S15), but the community-level plant nitrogen uptake rate (i.e. *Schizachyrium* and *Poa* together) showed no dependence on fine-root mass (Fig. 5b).

In the previously-published pot experiments (exp. 4), plant nitrogen uptake rates for individual seedlings were dependent on nitrogen availability (Fig. 6a, c), increased at small fine-root mass, and either saturated (Fig. 6a, c) or declined (Fig. 6b, d) at larger fine-root mass (Table 1). Data from Poorter et al. (1995) show a saturating relationship between plant nitrogen uptake rate and fine-root mass, with greater nitrogen uptake rates occurring at higher nitrogen availability (Fig. 6a, c). Data from Trinder et al. (2012) show an initially saturating relationship between fine-root mass and plant nitrogen uptake rate, with a decline in uptake rates at larger fine-root mass (Fig. 6b, d).

Previously published field studies 5

In previously-published field studies (exp. 5), plant community nitrogen uptake rate was most parsimoniously explained as linearly related to fine-root mass in the "Alaskan taiga" and "Aspen FACE" studies (Fig. 7a, b) and as independent of fine-root mass in the remaining five studies (Fig. 7c-g).

Discussion

We sought to determine the empirical relationship between plant community nitrogen uptake rate, nitrogen availability, and fine-root mass using a variety of new microcosm experiments (exps. 1 – 3),

372 reanalysis of published pot experiments (exp. 4), and published field observations (exp. 5). An important
373 goal was to empirically determine the most appropriate mathematical relationship for use in coupled
374 carbon-nitrogen terrestrial biosphere models (CN-TBMs, Fig. 1). Critically, these models attempt to
375 predict global climate change and thus the smallest scale of plants represented in CN-TBMs is usually
376 above the level of the individual. No single relationship was consistent with all of the results, which
377 implies that more work is needed to determine a generalizable model. However, in over 94% of the 39
378 microcosm and pot experimental conditions we considered (i.e. ignoring the field data for the moment),
379 plant community nitrogen uptake rate was either independent of fine-root mass entirely (67%) or
380 independent of fine-root mass across all but the lowest fine-root densities (i.e. saturating at low fine-root
381 mass, 28%). The two cases (5%) that showed a linear response had remarkably low fine-root mass (Fig.
382 4f,i). These responses occurred in communities of seedlings grown under semi-hydroponic conditions in
383 sand culture (exp. 1, Figs. 3, 5), communities of seedlings grown in soil (exp. 2, Fig. 4), and previously
384 published studies of individual seedlings grown in sand and soil (exp. 4, Fig. 6). Further, these results
385 were consistent with 70% of the field studies we reanalyzed from the literature (exp. 5, Fig. 7). The
386 studied taxa include a C3 grass, a C4 grass, several forbs, numerous temperate angiosperm tree species,
387 and numerous temperate and boreal gymnosperm tree species (Table 1). In all the cases where nitrogen
388 availability was manipulated (i.e. the microcosm and pot experiments 1 – 4), plant community nitrogen
389 uptake rate increased with increasing nitrogen availability (Figs. 3, 4, 6). Thus, of the three different
390 mathematical relationships currently used in coupled C-N TBMs (Fig. 1) to relate community nitrogen
391 uptake rate as a function of fine-root mass and nitrogen availability, our results generally support
392 *dependence* on nitrogen availability, but *independence* or *saturation* of fine-root mass (compare Fig. 1
393 with Figs. 3, 4, & 6).
394 The previously-published pot experiments (exp. 4) used a single seedling per pot and showed a
395 saturating response between plant nitrogen uptake and fine-root mass (Fig. 6), as did the one microcosm
396 experiment that only had one individual per pot (Fig. 4b). In a separate study that expressly manipulated

397 the density of seedlings while otherwise replicating the methods of the microcosm experiments presented
398 here, we found that one of two species (*Schizachyrium*) demonstrated a similar saturating response when
399 seedlings were grown in isolation (Fig. S17e) but not when grown at higher microcosm densities (Fig.
400 S17a,c). This suggests that plant *communities*, which are ubiquitous in nature, may have different uptake
401 responses than isolated plants, which are omnipresent in ecophysiology studies, even at the same total
402 fine-root mass. Even apart from those observations, it is likely that *all* of our results would have exhibited
403 a saturating response if we had started taking measurements when the plants had even smaller fine-root
404 systems. A plant community with no fine-root mass will take up no nitrogen, and the nitrogen uptake rate
405 must increase with fine-root mass from that starting point. Given both the observed saturating responses
406 and that logic, it is worth noting that in all saturating cases, the relationship saturated at fine-root mass
407 values (10 - 75 g m^{-2}) that are much lower than those observed in field studies. For comparison, of the 195
408 fine-root mass values reported in the FluxNet dataset of worldwide forested ecosystems (Luyssaert *et al.*,
409 2007), the minimum value is 68 g m^{-2}, the first quartile is 431 g m^{-2}, and the median is 614 g m^{-2}
410 (assuming biomass pools are approximately twice the reported carbon pools).
411 However, such comparisons between microcosm- and pot-grown seedlings and field-grown
412 adults may be questionable on numerous grounds, including differences in soil volume, environmental
413 conditions, ontogeny, and community composition (Poorter *et al.*, 2016). Thus, we also sought to
414 determine if our microcosm (exps. 1 – 3) and pot experiment (exp. 4) results were at least consistent with
415 field data from forest plots in seven published systems (exp. 5). Five were best fit by a model with no
416 fine-root dependence (compare Fig. 1a with Fig. 7c-g), though one of these (Pop-Euro FACE) was a
417 sapling plantation and may not be representative of most forests. Two systems were best fit by a model of
418 linear fine-root dependence (compare Fig. 1b with Fig. 7a,b). One of these (Aspen FACE) was a sapling
419 plantation with remarkably low fine-root mass, whereas the other surveyed plots in the Alaskan taiga.
420 Given their differing methodologies (Table S4) and limited independent information on nitrogen
421 availability or limitation by other resources (e.g. water, phosphorus), we should be careful not to over-

interpret the relationship between plant community nitrogen uptake rate, nitrogen availability (not independently measured and thus potentially confounded with fine-root mass), and fine-root mass from these field studies. With the exception of the Alaskan taiga and Aspen FACE studies (Fig. 7a,b), however, they do suggest that the microcosm and pot experiment results using seedlings are consistent with more ecological- and model-relevant field data at fine-root mass values expected for CN-TBMs.

Two other field studies have recently reported plant community nitrogen uptake rates that call into question a linear relationship between community nitrogen uptake rate and fine-root mass and are thus consistent with the majority of our results. Zhu *et al.* (2016) conducted an ^{15}N tracer study in tundra vegetation on three dominant plant species and found inconsistencies between their fine-root mass profiles by depth, the ammonium pool size by depth, and their ^{15}N uptake rates by depth, suggesting a decoupling of community nitrogen uptake rates and fine-root mass. Kulmatiski *et al.* (2017) conducted a dual water and nitrogen tracer study using five dominant species in sagebrush-steppe ecosystem and, like Zhu *et al.*, found inconsistencies between fine-root mass profiles by depth, water & nitrogen availability by depth, and tracer uptake rates by depth. Although fine-root mass was not predictive, resource uptake rates were positively correlated with resource availability (Kulmatiski *et al.*, 2017), consistent with the results of the different nitrogen levels applied to the microcosms and pots in the experiments reported here.

Implications for coupled carbon-nitrogen terrestrial biosphere models

There are two general approaches used to represent vegetation structure in CN-TBMs: vegetation that is prescribed at the stand-level (i.e. community-level) and vegetation that is determined via dynamic competition. Our results bear differently on these two approaches. Taken together, we find little empirical evidence to support inclusion of fine-root mass in the calculation of nitrogen uptake rates for *stand-level* CN-TBMs. There is evidence of a saturating relationship between fine roots and nitrogen uptake, but saturation occurs at very low fine-root mass (< 75 g/m2) not commonly observed in grassland or forest

ecosystems. By including fine-root dependence, stand-level CN-TBMs effectively introduce a parameter (or in the case of a saturating relationship, two parameters) that is unnecessary, needlessly increasing model complexity and uncertainty. Furthermore, it *forces* an unfounded relationship between belowground carbon allocation and nitrogen uptake rates if – as supported by the results presented here – there is no strong relationship between plant community nitrogen uptake rate and fine-root mass at field-relevant values.

This result grinds against intuition that more root production at the individual level should equal more uptake capacity. Indeed, our two-species replacement series microcosm experiment (exp. 3) demonstrated that having a greater fraction of the community root mass will lead to a greater share of nitrogen uptake (Fig. 5a). At the same time, however, the *community-level* nitrogen uptake rate was unaffected by fine-root mass (Fig. 5b). Thus, we suggest that CN-TBMs that *do* explicitly model belowground competition (e.g. Weng *et al.*, 2015, Weng *et al.*, 2017) should scale *individual* plant nitrogen uptake rates by the individual's fine-root mass *relative* to community-level fine-root mass, multiplied by nitrogen availability (Dybzinski *et al.*, 2011, Dybzinski *et al.*, 2015, McNickle *et al.*, 2016, Weng *et al.*, 2017). Fine-root mass may be prescribed as a trait of a given plant functional type, or, better, solved as an evolutionarily stable strategy (ESS), i.e. by determining the resident fine-root mass for which no alternative individual-level fine-root mass would be more competitive (Weng *et al.*, 2015, Weng *et al.*, 2017). In addition, models that explicitly include rhizosphere priming effects may benefit from the inclusion of *absolute* fine-root mass in nitrogen uptake rate functions, but only for the fraction of nitrogen made available by priming (Cheng *et al.*, 2013).

A game-theoretic interpretation of the results

How do our results, which suggest that plant community nitrogen uptake rate was largely independent of fine-root mass (Figs. 3, 4, 6), even though nitrogen was limiting (Figs. S2 & S8), square with observations of fine-root mass (or its correlates) changing consistently along environmental

gradients? Fine-root mass and/or fine-root mass usually decreases in response to experimental nitrogen additions (Li *et al.*, 2015) and usually increases in patches of relatively higher nitrogen availability (Hodge, 2004). *Why would fine-root mass change in such predictable ways if fine-root mass does not limit nitrogen uptake rates?* One possibility is that nitrogen availability gradients may be correlated with other limiting resources, such as light, water, or phosphorus, that are the true determinants of fine-root allocation. However, this would not explain the differential fine-root mass responses in experiments that manipulated nitrogen and other resources (Gower *et al.*, 1992, Jackson *et al.*, 2009, Farrior *et al.*, 2013). Moreover, in our experiment, all other resources (light, water, and macro- and micronutrients) were provided in equal and abundant measure across treatments. Because the low-nitrogen plants were smaller, they had *relatively more* macro- and micro-nutrients available to them per unit plant mass and had to move *less* water to maximize photosynthetic rates, making it improbable that they were limited by any other belowground resource.

These two observations, that fine-root mass often changes in predictable ways across environmental gradients (e.g. citations above), and that plant community nitrogen uptake rate appears independent of fine-root mass (i.e. this study), are not mutually exclusive. Indeed, they are predicted by game-theoretic models of individual-based plant competition for nitrogen (Gersani *et al.*, 2001, Dybzinski *et al.*, 2011, Farrior *et al.*, 2013, McNickle & Dybzinski, 2013, Dybzinski *et al.*, 2015, McNickle *et al.*, 2016), in which natural selection is seen to favor plants that "over-proliferate" their fine roots for competitive reasons. Although the flux of nitrogen controlled by soil microbial decomposition and taken up by the plant community may be fixed and unaffected by *community-level* fine-root mass (Fig. 5b), an advantage goes to an *individual* with more fine roots than its neighbors because it gains a greater *share* through diffusion and mass flow (Fig. 5a) and thus "preempts" nitrogen that would have otherwise gone to its neighbors (Zhang *et al.*, 1999, Gersani *et al.*, 2001, Craine *et al.*, 2005). Put colloquially, the individual with relatively more roots gets a bigger *share* of the pie; it doesn't change the *size* of the pie (the decomposers control the size of the pie). The value of that bigger share of the pie relative to the cost

of building additional fine roots determines the competitive investment in fine-root mass *and thus changes with available nitrogen and other ecological circumstances despite no change in plant community nitrogen uptake rate with community-level fine-root mass*. Thus, uptake rates per unit root, rather than being constant, may change in different contexts. Using very different game theoretic models, Dybzinski *et al.* (2011), Dybzinski *et al.* (2015), and McNickle *et al.* (2016) predicted that the ESS fine-root mass for nitrogen-limited trees should *decrease* with increasing nitrogen availability and *increase* with increasing atmospheric [CO_2]. This occurs because the marginal benefits of nitrogen allocated to light-limited photosynthesis *decrease* with increasing nitrogen availability (due to greater LAI) and *increase* with increasing atmospheric [CO_2] (due to greater photosynthetic efficiency). Such mechanistic "stopping rules" derived from competition theory could be used to determine fine-root allocation in stand-level CN-TBMs or other higher-level models that are not explicitly competitive.

It is perhaps useful to note that fine-root over-proliferation may be, to some extent, a *fixed* trait among many contemporary plant species because of their consistent evolutionary history of competition (McNickle & Dybzinski, 2013). Fine root over-proliferation may also be, to some extent, a *plastic* trait among many contemporary plant species because of their inconsistent evolutionary history of competition, in which individuals that could perceive and respond to competitors via over-proliferation benefited by not over-proliferating in the absence of competition (McNickle & Dybzinski, 2013). An analogy aboveground may be helpful: many plants (trees included) will grow tall even when grown in isolation (a fixed response), but many plants will also grow taller if they perceive a shift in the red to far-red ratio consistent with the presence of competitors (a plastic response) (Dudley & Schmitt, 1996). Thus, it seems reasonable to believe that the saturation of the nitrogen uptake rate with fine-root mass exhibited in the pot experiments that used single individuals (Figs. 4b, 6, S17e) reflects a fixed component of fine root over-proliferation, whereas the independence of the nitrogen uptake rate with fine-root mass exhibited in the microcosm experiments that used many individuals (Figs. 3, 4 (all but b), 5) reflects both fixed and plastic components of fine-root over-proliferation. Indeed, density, species

identity, and intra- versus inter-specific interactions all have the potential to change the plastic fine-root over-proliferation response.

Caveats and questions for future research

Our method for determining the nitrogen uptake rate in experiments 1 – 4 relies on the use of seedlings, the only plant stage for which it is safe to assume that nitrogen loss rates are negligible compared to nitrogen uptake rates. Thus, an important caveat of our method and results is that ontogeny is conflated with our measure of nitrogen uptake rate as a function of fine-root mass: the smaller fine-root masses are from smaller, younger plants, and the larger fine-root masses are from larger, older plants. Indeed, nitrogen uptake rates at higher fine-root mass values (i.e. older plants) sometimes declined (e.g. Figs. 3a,b, 4n, 6b,d), indicating that the assumption that nitrogen losses are negligible was likely violated in these older plants. We cannot reject the possibility that changes in root physiology over time affected our results. However, results from a separate study that manipulated seedling density show that ontogeny had little, if any, effect on the results (Fig. S18): for fine-root mass greater than approximately 50 g m^{-2}, microcosms harvested on the same day with differences in fine-root mass attributable to different planting densities showed an obvious relationship between plant community nitrogen uptake rate and nitrogen availability but no consistent relationship between plant community nitrogen uptake rate and fine-root mass. Moreover, a rejection of our conclusions based on methodological concerns about greenhouse microcosm and pot studies, understandable as they are, would be unwarranted given that data synthesized from a series of field studies (Fig. 7) and two published field tracer studies (Zhu *et al.*, 2016, Kulmatiski *et al.*, 2017) are largely consistent with the greenhouse microcosm and pot experiment results, as discussed above.

Additional factors have the potential to alter or refine the conclusions presented here, including relationships between fine-root mass and the rhizosphere community, connections between nitrogen uptake rate and other fine-root traits, and possible dependence of other soil resource uptake rates on fine-

547 root mass. Although we did not sterilize our substrate or attempt to exclude microbes, our methodology
548 likely omitted any substantial interactions with mycorrhizal fungi, which are known to play an important
549 role in soil nitrogen cycling (Schimel & Bennett, 2004). Thus, it remains an open question to what extent
550 the presence of an established mycorrhizal network might change the relationship between plant
551 community nitrogen uptake rate, nitrogen availability, and fine-root mass found in this study. Similarly,
552 the lack of an established soil community may have affected the influence of rhizosphere priming effects
553 (Phillips *et al.*, 2012), which might be expected to scale linearly with fine-root mass. Nor did we measure
554 other morphological or architectural root traits, such as fine-root area, fine-root length, root hair density,
555 branching ratio, branching intensity, root tip density, etc. (McCormack *et al.*, 2017). Although our
556 measure of fine-root mass is certainly appropriate for CN-TBMs, these other traits are more directly
557 linked to fine-root function. Thus, future studies that replicate our methodology but that also measure
558 these fine-root traits may yield insights that are not possible by measures of fine-root mass alone. Note
559 that any insights different than those presented here would necessarily require that the alternative fine-
560 root trait scales non-linearly with fine-root mass. If it scaled linearly, the results would be qualitatively
561 identical to those presented here for fine-root mass. Anecdotally, we noted no visible change in fine-root
562 diameter across harvests within a given species. Finally, we focused on nitrogen exclusively; we can say
563 nothing about whether uptake rates of other belowground resources, many of which may be more
564 diffusion-limited (e.g. phosphorus), depend on fine-root mass. Nor can we say whether interactions
565 between limiting resources and/or luxury uptake (Wright *et al.*, 2003, Agren, 2008, Sistla *et al.*, 2015)
566 may depend on fine-root mass.
567
568 *Final remarks*
569 In the absence of data relating nitrogen availability, fine-root mass, and nitrogen uptake rate,
570 coupled carbon-nitrogen terrestrial biosphere models (CN-TBMs) have either assumed no dependence,
571 linear dependence, or saturating dependence on fine-root mass (Fig. 1). Because fine roots are responsible

for capturing nitrogen, CN-TBMs that include fine-root dependence may be considered a mechanistic advance (Matamala & Stover, 2013, Ghimire *et al.*, 2016), but the results presented here suggest that CN-TBMs that model vegetation at the community-level might be more accurate if they omit fine-root mass in nitrogen uptake equations. We determined the empirical relationship between these variables for 46 unique combinations of species, nitrogen levels, and growing conditions, and the results provide support for models whose plant community nitrogen uptake rates depend on nitrogen availability but not on fine-root mass. In contrast to most existing CN-TBMs, CN-TBMs that explicitly include competition for donor-controlled soil resources, along with the necessary individual-level competition, *should* include *relative* fine-root mass for competitive reasons (e.g. Weng *et al.*, 2015, Weng *et al.*, 2017). We believe such an approach has the potential to link the carbon and nitrogen cycles in a more mechanistically-realistic way.

Acknowledgements

We gratefully acknowledge funding from Loyola University Chicago; suggestions for improvement by David Robinson and anonymous peer reviewers; logistical support from K. Erickson; help with maintenance and harvests from O. Urbanski, L. Papaioannou, H. Roudebush, & V. Roudebush; and tissue and substrate analyses from Z. Zhu. The authors have no conflicts of interest to report.

References

Agren GI (2008) Stoichiometry and Nutrition of Plant Growth in Natural Communities. *Annual Review of Ecology Evolution and Systematics,* **39**, 153-170.

Bassirirad H (2000) Kinetics of nutrient uptake by roots: responses to global change. *New Phytologist,* **147**, 155-169.

Bolker BM, R Core Team (2017) bbmle: Tools for General Maximum Likelihood Estimation.

Cavanaugh JE (1997) Unifying the derivations for the Akaike and corrected Akaike information criteria. *Statistics & Probability Letters,* **33**, 201-208.

Cheng WX, Parton WJ, Gonzalez-Meler MA *et al.* (2013) Synthesis and modeling perspectives of rhizosphere priming. *New Phytologist,* **201**, 31-44.

Comins HN, Mcmurtrie RE (1993) Long-Term Response of Nutrient-Limited Forests to Co2 Enrichment - Equilibrium Behavior of Plant-Soil Models. *Ecological Applications,* **3**, 666-681.

603 Cottingham KL, Lennon JT, Brown BL (2005) Knowing when to draw the line: designing more
604 informative ecological experiments. *Frontiers in Ecology and the Environment,* **3**, 145-
605 152.
606 Craine JM (2006) Competition for nutrients and optimal root allocation. *Plant and Soil,* **285**, 171-
607 185.
608 Craine JM, Fargione J, Sugita S (2005) Supply pre-emption, not concentration reduction, is the
609 mechanism of competition for nutrients. *New Phytologist,* **166**, 933-940.
610 Dudley SA, Schmitt J (1996) Testing the adaptive plasticity hypothesis: Density-dependent
611 selection on manipulated stem length in Impatiens capensis. *American Naturalist,* **147**,
612 445-465.
613 Dybzinski R, Farrior C, Wolf A, Reich PB, Pacala SW (2011) Evolutionarily Stable Strategy
614 Carbon Allocation to Foliage, Wood, and Fine Roots in Trees Competing for Light and
615 Nitrogen: An Analytically Tractable, Individual-Based Model and Quantitative
616 Comparisons to Data. *American Naturalist,* **177**, 153-166.
617 Dybzinski R, Farrior CE, Pacala SW (2015) Increased forest carbon storage with increased
618 atmospheric CO2 despite nitrogen limitation: a game-theoretic allocation model for trees
619 in competition for nitrogen and light. *Global Change Biology,* **21**, 1182-1196.
620 Falster DS, Westoby M (2003) Plant height and evolutionary games. *Trends in Ecology &*
621 *Evolution,* **18**, 337-343.
622 Farrior CE, Tilman D, Dybzinski R, Reich PB, Levin SA, Pacala SW (2013) Resource limitation
623 in a competitive context determines complex plant responses to experimental resource
624 additions. *Ecology,* **94**, 2505-2517.
625 Finzi AC, Norby RJ, Calfapietra C *et al.* (2007) Increases in nitrogen uptake rather than
626 nitrogen-use efficiency support higher rates of temperate forest productivity under
627 elevated CO2. *Proceedings of the National Academy of Sciences of the United States of*
628 *America,* **104**, 14014-14019.
629 Fisher RA, Koven CD, Anderegg WRL *et al.* (2018) Vegetation demographics in Earth System
630 Models: A review of progress and priorities. *Global Change Biology,* **24**, 35-54.
631 Fisher RA, Muszala S, Verteinstein M *et al.* (2015) Taking off the training wheels: the properties
632 of a dynamic vegetation model without climate envelopes, CLM4.5(ED). *Geoscientific*
633 *Model Development,* **8**, 3593-3619.
634 Garnier E (1991) Resource Capture, Biomass Allocation and Growth in Herbaceous Plants.
635 *Trends in Ecology & Evolution,* **6**, 126-131.
636 Gerber S, Hedin LO, Keel SG, Pacala SW, Shevliakova E (2013) Land-use change and nitrogen
637 feedbacks constrain the trajectory of the land carbon sink. *Geophysical Research*
638 *Letters*, 2013GL057260.
639 Gerber S, Hedin LO, Oppenheimer M, Pacala SW, Shevliakova E (2010) Nitrogen cycling and
640 feedbacks in a global dynamic land model. *Global Biogeochem. Cyc.,* **24**.
641 Gersani M, Brown JS, O'brien EE, Maina GM, Abramsky Z (2001) Tragedy of the commons as a
642 result of root competition. *Journal of Ecology,* **89**, 660-669.
643 Ghimire B, Riley WJ, Koven CD, Mu MQ, Randerson JT (2016) Representing leaf and root
644 physiological traits in CLM improves global carbon and nitrogen cycling predictions.
645 *Journal of Advances in Modeling Earth Systems,* **8**, 598-613.
646 Givnish TJ (1982) On the Adaptive Significance of Leaf Height in Forest Herbs. *American*
647 *Naturalist,* **120**, 353-381.
648 Gower ST, Vogt KA, Grier CC (1992) Carbon dynamics of Rocky mountain douglas-fir:
649 Influence of water and nutrient availability. *Ecological Monographs,* **62**, 43-65.
650 Hodge A (2004) The plastic plant: root responses to heterogeneous supplies of nutrients. *New*
651 *Phytologist,* **162**, 9-24.

Huang S, Arain MA, Arora VK, Yuan FM, Brodeur J, Peichl M (2011) Analysis of nitrogen controls on carbon and water exchanges in a conifer forest using the CLASS-CTEMN+ model. *Ecological Modelling,* **222**, 3743-3760.

Hughes AP, Freeman PR (1967) Growth Analysis Using Frequent Small Harvests. *Journal of Applied Ecology,* **4**, 553-560.

Hungate BA, Dukes JS, Shaw MR, Luo YQ, Field CB (2003) Nitrogen and climate change. *Science,* **302**, 1512-1513.

Jackson RB, Cook CW, Pippen JS, Palmer SM (2009) Increased belowground biomass and soil CO2 fluxes after a decade of carbon dioxide enrichment in a warm-temperate forest. *Ecology,* **90**, 3352-3366.

Kronzucker HJ, Siddiqi MY, Glass ADM (1995) Kinetics of No3- Influx in Spruce. *Plant Physiology,* **109**, 319-326.

Kulmatiski A, Adler PB, Stark JM, Tredennick AT (2017) Water and nitrogen uptake are better associated with resource availability than root biomass. *Ecosphere,* **8**.

Lebauer DS, Treseder KK (2008) Nitrogen limitation of net primary productivity in terrestrial ecosystems is globally distributed. *Ecology,* **89**, 371-379.

Li WB, Jin CJ, Guan DX, Wang QK, Wang AZ, Yuan FH, Wu JB (2015) The effects of simulated nitrogen deposition on plant root traits: A meta-analysis. *Soil Biology & Biochemistry,* **82**, 112-118.

Lichstein JW, Golaz NZ, Malyshev S *et al.* (2014) Confronting terrestrial biosphere models with forest inventory data. *Ecological Applications,* **24**, 699-715.

Luyssaert S, Inglima I, Jung M *et al.* (2007) CO2 balance of boreal, temperate, and tropical forests derived from a global database. *Global Change Biology,* **13**, 2509-2537.

Matamala R, Stover DB (2013) Introduction to a Virtual Special Issue: modeling the hidden half - the root of our problem. *New Phytologist,* **200**, 939-942.

Mccormack ML, Guo D, Iversen CM *et al.* (2017) Building a better foundation: improving root-trait measurements to understand and model plant and ecosystem processes. *New Phytologist*, n/a-n/a.

Mcnickle GG, Dybzinski R (2013) Game theory and plant ecology. *Ecology Letters,* **16**, 545-555.

Mcnickle GG, Gonzalez-Meler MA, Lynch DJ, Baltzer JL, Brown JS (2016) The world's biomes and primary production as a triple tragedy of the commons foraging game played among plants. *Proceedings of the Royal Society B-Biological Sciences,* **283**.

Nadelhoffer KJ, Aber JD, Melillo JM (1985) Fine roots, net primary production, and soil nitrogen availability: a new hypothesis. *Ecology,* **66**, 1377-1390.

Norby RJ, Delucia EH, Gielen B *et al.* (2005) Forest response to elevated CO2 is conserved across a broad range of productivity. *Proceedings of the National Academy of Sciences of the United States of America,* **102**, 18052-18056.

Oleson K, Lawrence D, Bonan G *et al.* (2013) Technical description of version 4.5 of the Community Land Model (CLM). pp 422, Boulder, CO, Natl. Cent. for Atmos. Res.

Peñuelas J, Poulter B, Sardans J *et al.* (2013) Human-induced nitrogen–phosphorus imbalances alter natural and managed ecosystems across the globe. *Nat Commun,* **4**.

Phillips RP, Meier IC, Bernhardt ES, Grandy AS, Wickings K, Finzi AC (2012) Roots and fungi accelerate carbon and nitrogen cycling in forests exposed to elevated CO2. *Ecology Letters,* **15**, 1042-1049.

Poorter H, Fiorani F, Pieruschka R *et al.* (2016) Pampered inside, pestered outside? Differences and similarities between plants growing in controlled conditions and in the field. *New Phytologist,* **212**, 838-855.

Poorter H, Van De Vijver Claudius ADM, Boot Rene GA, Lambers H (1995) Growth and carbon economy of a fast-growing and a slow-growing grass species as dependent on nitrate supply. *Plant & Soil,* **171**, 217-227.

R Core Team (2015) R: A language and environment for statistical computing. *R Foundation for Statistical Computing, Vienna, Austria. URL:* http://www.R-project.org/.

Raich JW, Rastetter EB, Melillo JM *et al.* (1991) Potential Net Primary Productivity in South-America - Application of a Global-Model. *Ecological Applications,* **1**, 399-429.

Ruess RW, Vancleve K, Yarie J, Viereck LA (1996) Contributions of fine root production and turnover to the carbon and nitrogen cycling in taiga forests of the Alaskan interior. *Canadian Journal of Forest Research-Revue Canadienne De Recherche Forestiere,* **26**, 1326-1336.

Schimel JP, Bennett J (2004) Nitrogen mineralization: Challenges of a changing paradigm. *Ecology,* **85**, 591-602.

Sistla SA, Appling AP, Lewandowska AM, Taylor BN, Wolf AA (2015) Stoichiometric flexibility in response to fertilization along gradients of environmental and organismal nutrient richness. *Oikos,* **124**, 949-959.

Smith B, Warlind D, Arneth A, Hickler T, Leadley P, Siltberg J, Zaehle S (2014) Implications of incorporating N cycling and N limitations on primary production in an individual-based dynamic vegetation model. *Biogeosciences,* **11**, 2027-2054.

Tateno R, Hishi T, Takeda H (2004) Above- and belowground biomass and net primary production in a cool-temperate deciduous forest in relation to topographical changes in soil nitrogen. *Forest Ecology and Management,* **193**, 297-306.

Tateno R, Takeda H (2010) Nitrogen uptake and nitrogen use efficiency above and below ground along a topographic gradient of soil nitrogen availability. *Oecologia,* **163**, 793-804.

Thornton PE, Lamarque JF, Rosenbloom NA, Mahowald NM (2007) Influence of carbon-nitrogen cycle coupling on land model response to CO(2) fertilization and climate variability. *Global Biogeochem. Cyc.,* **21**.

Tinker PH, Nye PB (2000) *Solute movement in the rhizosphere,* New York, Oxford University Press.

Trinder C, Brooker R, Davidson H, Robinson D (2012) Dynamic trajectories of growth and nitrogen capture by competing plants. *New Phytologist,* **193**, 948-958.

Van Der Werf A, Visser AJ, Schieving F, Lambers H (1993) Evidence for optimal partitioning of biomass and nitrogen at a range of nitrogen availability for a fast- and a slow-growing species. *Functional Ecology,* **7**, 63-74.

Wang S, Grant RF, Verseghy DL, Black TA (2001) Modelling plant carbon and nitrogen dynamics of a boreal aspen forest in CLASS - the Canadian Land Surface Scheme. *Ecological Modelling,* **142**, 135-154.

Wang YP, Houlton BZ (2009) Nitrogen constraints on terrestrial carbon uptake: Implications for the global carbon-climate feedback. *Geophysical Research Letters,* **36**.

Wang YP, Law RM, Pak B (2010) A global model of carbon, nitrogen and phosphorus cycles for the terrestrial biosphere. *Biogeosciences,* **7**, 2261-2282.

Warren JM, Hanson PJ, Iversen CM, Kumar J, Walker AP, Wullschleger SD (2015) Root structural and functional dynamics in terrestrial biosphere models - evaluation and recommendations. *New Phytologist,* **205**, 59-78.

Weng E, Farrior CE, Dybzinski R, Pacala SW (2017) Predicting vegetation type through physiological and environmental interactions with leaf traits: evergreen and deciduous forests in an earth system modeling framework. *Global Change Biology,* **23**, 2482–2498.

Weng ES, Malyshev S, Lichstein JW *et al.* (2015) Scaling from individual trees to forests in an Earth system modeling framework using a mathematically tractable model of height-structured competition. *Biogeosciences,* **12**, 2655-2694.

Woodward FI, Smith TM, Emanuel WR (1995) A Global Land Primary Productivity and Phytogeography Model. *Global Biogeochem. Cyc.,* **9**, 471-490.

Wright IJ, Reich PB, Westoby M (2003) Least-cost input mixtures of water and nitrogen for photosynthesis. *American Naturalist,* **161**, 98-111.

Yang XJ, Wittig V, Jain AK, Post W (2009) Integration of nitrogen cycle dynamics into the Integrated Science Assessment Model for the study of terrestrial ecosystem responses to global change. *Global Biogeochem. Cyc.,* **23**.

Zaehle S, Friend AD (2010) Carbon and nitrogen cycle dynamics in the O-CN land surface model: 1. Model description, site-scale evaluation, and sensitivity to parameter estimates. *Global Biogeochem. Cyc.,* **24**.

Zaehle S, Friend AD, Friedlingstein P, Dentener F, Peylin P, Schulz M (2010) Carbon and nitrogen cycle dynamics in the O-CN land surface model: 2. Role of the nitrogen cycle in the historical terrestrial carbon balance. *Global Biogeochem. Cyc.,* **24**.

Zaehle S, Medlyn BE, De Kauwe MG *et al.* (2014) Evaluation of 11 terrestrial carbon-nitrogen cycle models against observations from two temperate Free-Air CO2 Enrichment studies. *New Phytologist,* **202**, 803-822.

Zhang DY, Sun GJ, Jiang XH (1999) Donald's ideotype and growth redundancy: a game theoretical analysis. *Field Crops Research,* **61**, 179-187.

Zhu Q, Iversen CM, Riley WJ, Slette IJ, Vander Stel HM (2016) Root traits explain observed tundra vegetation nitrogen uptake patterns: Implications for trait-based land models. *Journal of Geophysical Research-Biogeosciences,* **121**, 3101-3112.

Tables

Table 1. Summary of most parsimonious fits by AICc to experimental and observational data: Mean = grand mean (Fig. 1a); Linear = zero-intercept linear (Fig. 1b); Sat. = zero-intercept saturating (Fig. 1c).

		Sand culture microcosm and pot experiments			Soil culture microcosm and pot experiments				Figs. & Grand Total	Exp. #
Species or habitat	**Form***	**Low N**	**Med N**	**High N**	**Low N**	**Med N**	**High N**	**Field Obs.**		
Betula papyrifera	Ang. tree						Mean		4a	2
Acer rubrum	Ang. tree				Sat.		Sat.		4b	2
Liquidambar styraciflua (+ORNL FACE)	Ang. tree				Mean		Mean	Mean	4c, 7g	2, 5
Robinia pseudoacacia	Ang. tree						Sat.		4d	2
Pop-Euro FACE (Populus spp.)	Ang. trees							Mean	7e	5
Aspen FACE (Populus, Acer, Betula spp.)	Ang. trees							Linear	7b	5
Alaska taiga	Mixed trees							Linear	7a	5
Wisconsin temperate	Mixed trees							Mean	7c	5
Japan deciduous	Mixed trees							Mean	7f	5
Pinus sylvestris	Gym. tree	Mean	Mean	Mean	Mean		Mean		3a, 4n	1, 2
Picea abies	Gym. tree				Sat.		Mean		4h	2
Picea glauca	Gym. tree				Linear		Sat.		4i	2
Pinus taeda (+Duke FACE)	Gym. tree				Sat.		Mean/Sat.	Mean	4j, 7d	2, 5
Pinus banksiana	Gym. tree				Mean		Mean		4k	2
Pinus resinosa	Gym. tree				Mean		Mean		4l	2
Pinus strobus	Gym. tree				Mean		Sat.		4m	2
Poa pratensis	C3 grass	Mean	Mean	Mean	Sat.		Mean		3c, 4g	1, 2
Holcus lanatus	C3 grass	Sat.		Sat.					6c	4
Deschampsia flexuosa	C3 grass	Sat.		Sat.					6a	4
Dactylis glomerata	C3 grass					Mean/Sat.			6d	4
Schizachyrium scoparium	C4 grass	Mean	Mean	Mean	Linear		Mean		3b, 4f	1, 2
Trifolium pretense	Forb						Mean		4e	2
Plantago lanceolata	Forb					Mean/Sat.			6b	4
Summary		Mean: 3 Linear 0 Sat.: 2	Mean: 3 Linear 0 Sat.: 0	Mean: 3 Linear 0 Sat.: 2	Mean: 5 Linear 2 Sat.: 4	Mean: 2 Linear: 0 Sat.: 2	Mean: 10 Linear: 0 Sat.: 4	Mean: 5 Linear: 2 Sat.: 0	**Mean: 31** **Linear: 4** **Sat.: 14**	

*Ang. = Angiosperm; Gym. = Gymnosperm

Figures

Figure 1. The predominant assumptions in terrestrial biosphere models linking plant nitrogen uptake with nitrogen availability and fine-root mass: mean (independence of fine-root mass, a), linear (multiplicative dependence on fine-root mass, b), or saturating (multiplicative and saturating dependence on fine-root mass, c). Examples of models that use each assumption are provided (see Table S1 for references).

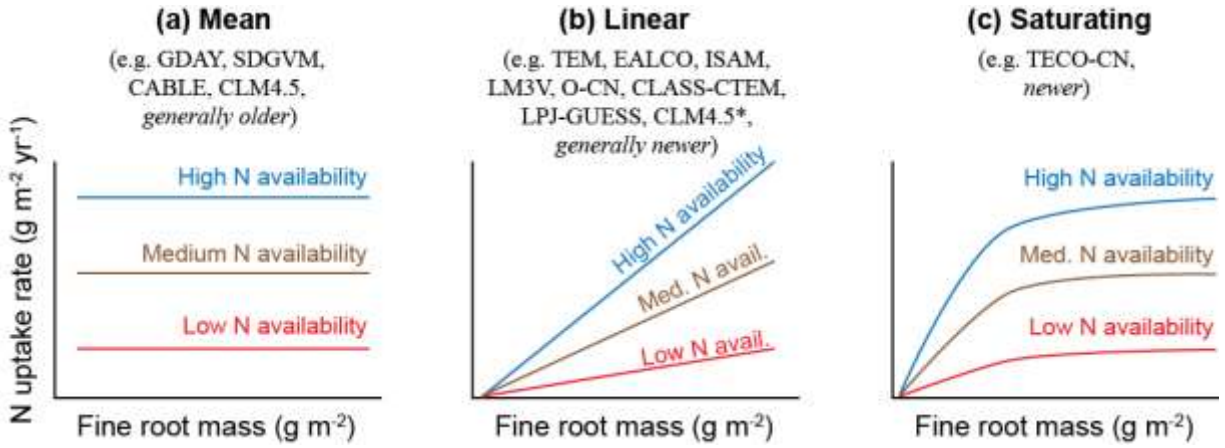

Figure 2. Mock data and an overview of the method used to relate nitrogen uptake rate to root mass (c) for our microcosm experiments (both sand culture and soil) and for our reanalysis of previously published pot experiment data. The nitrogen uptake rate is calculated as the derivative of total plant nitrogen uptake with respect to time (a), and root mass is taken as its predicted value from the data (b). Data that generated three example data points in (c) are highlighted in (a) and (b) (pink, green, and purple). Finally, we use maximum likelihood methods and AICc scores to find the most parsimonious model from among the three models shown in Fig. 1: mean, $NUR = c$; linear with zero intercept, $NUR = mR$; and saturating with zero intercept, $NUR = \frac{vR}{k+R}$. For the mock data shown (d, e), the linear model is the most parsimonious (where ΔAICc measures the difference between a given model's AICc and the lowest AICc of all the models). Because the saturating model can approximate both the mean model ($k = 0$) and the linear model ($k \gg R$), it will invariably fit the data as good or better than the mean or linear models, but the saturating model has an extra parameter penalty in AICc. For the mock data shown, the saturating fit is nearly identical to the linear fit (it is slightly offset in the figure so that both lines can be seen).

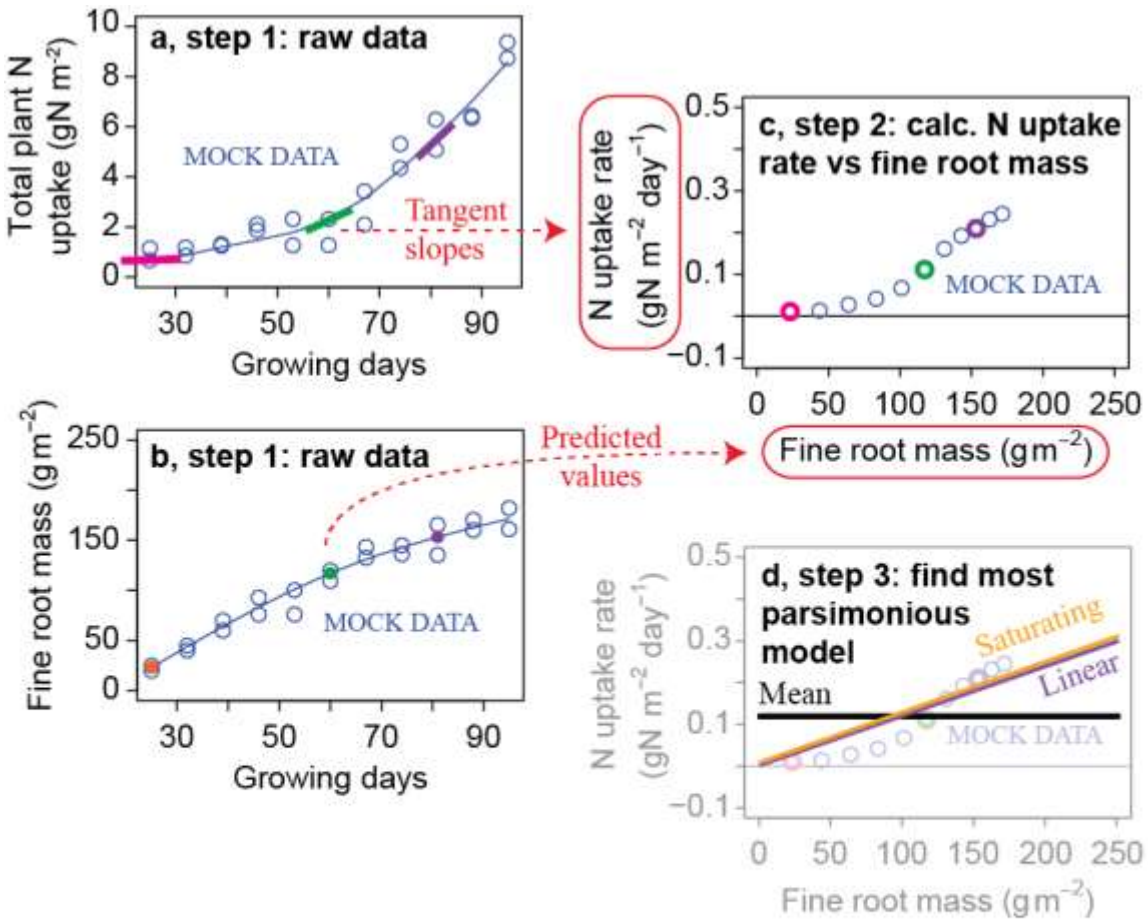

e, step 3: find most parsimonious model

	AICc	ΔAICc	df
Linear	-35.3	0	1
Saturating	-31.3	4	2
Mean	-17.0	18.3	1

Most parsimonius model

Figure 3. **Sand culture microcosm experiment (exp. 1)**: plant community nitrogen uptake rate versus fine-root mass. Lines show 500 bootstrapped relationships per species per nitrogen level. Bootstrap colors represent nitrogen application rate: red = low (0.057 mgN d^{-1}); brown = medium (0.237 mgN d^{-1}); and blue = high (1.139 mgN d^{-1}), with black symbols used for actual data (see Fig. 2). Most parsimonious fits by AICc: M = grand mean (Fig. 1a).

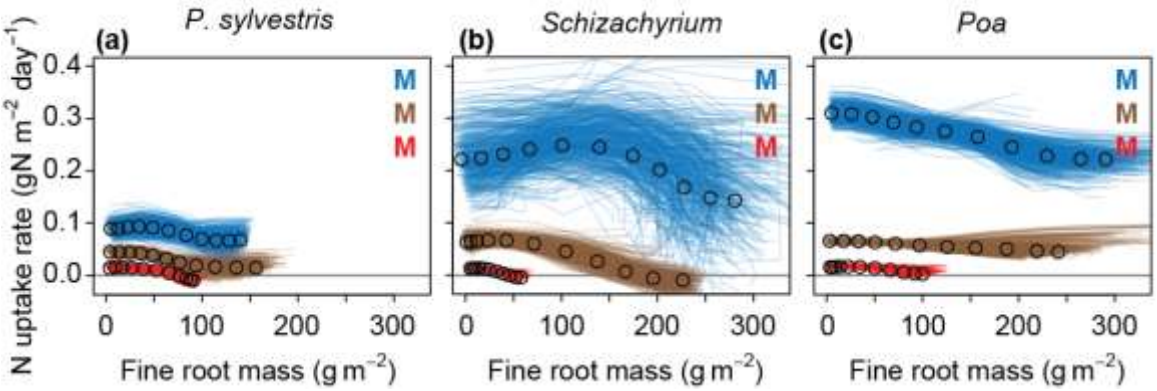

Figure 4. **Soil microcosm experiment (exp. 2)**: plant community nitrogen uptake rate versus fine-root mass for angiosperms (a-g) and gymnosperms (h-n) (see Methods for species details). Lines show 500 bootstrapped relationships per species per soil fertility level. Bootstrap colors represent soil fertility: red = low, blue = high, with black symbols used for actual data (see Fig. 2). Most parsimonious fits by AICc: M = grand mean (Fig. 1a); L = zero-intercept linear (Fig. 1b); S = zero-intercept saturating (Fig. 1c); M/S = grand mean and zero-intercept saturating are equally parsimonious (i.e. $\Delta AICc \leq 2$).

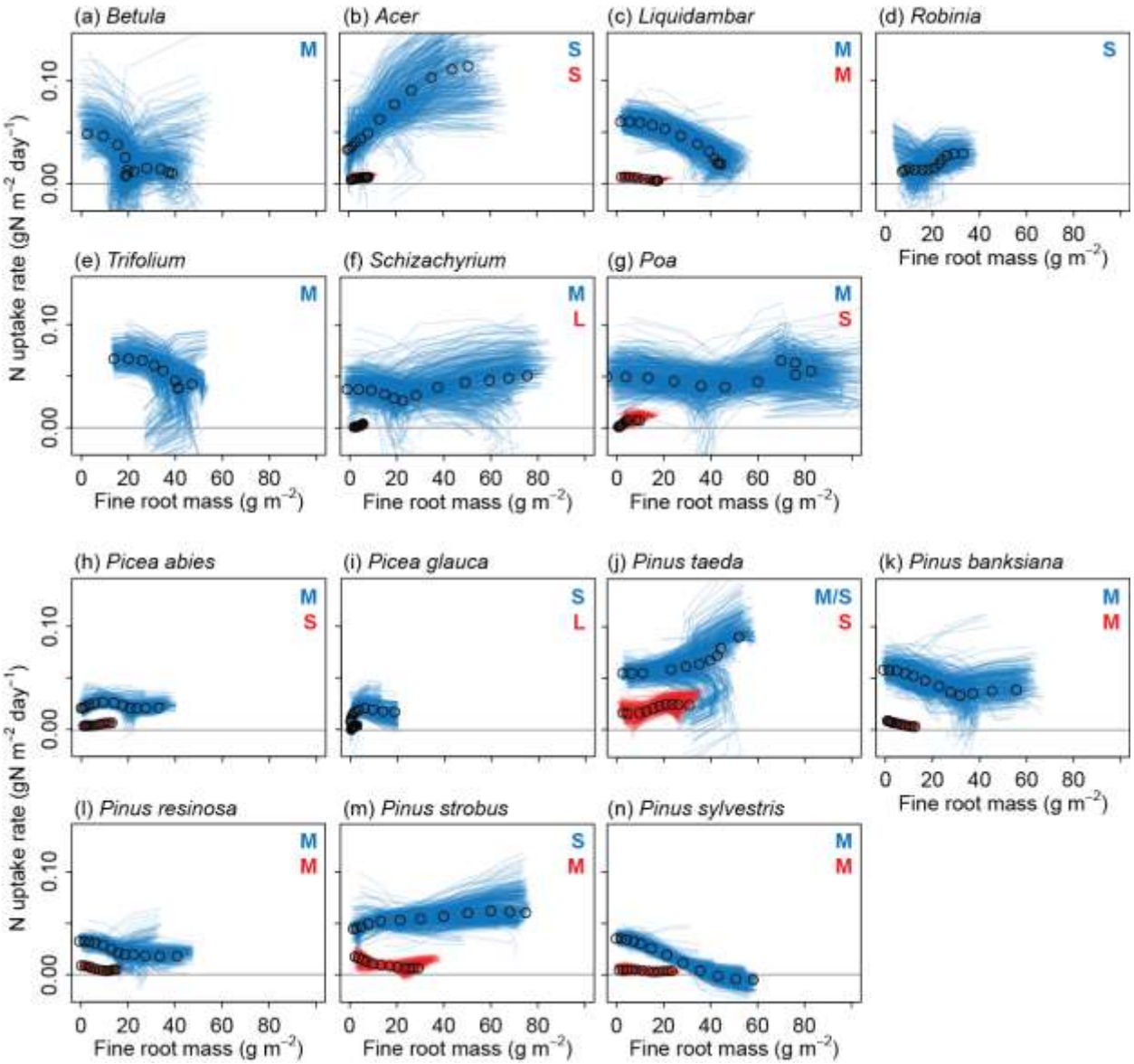

Figure 5. **Sand culture two-species replacement series experiment (exp. 3):** For microcosms of *Schizachyrium* and *Poa* growing together at different ratios, the fraction of nitrogen taken up by the population of *Schizachyrium* individuals versus their fraction of fine-root mass (a). This shows harvests 1 – 4, when root mass could be unambiguously separated to species, $r = 0.91$, p-value $< 10^{-6}$, although all harvests show this relationship (Fig. S15). The fractions for *Poa* in (a) are just the mirror image of the fractions for *Schizachyrium* reflected around the 1:1 line and thus they are not shown. Plant community nitrogen uptake rate (both species combined) versus fine-root mass (both species combined) is also shown (b). In b, lines show 500 bootstrapped relationships, with black symbols used for actual data (see Fig. 2). Most parsimonious fit by AICc: M = grand mean (Fig. 1a).

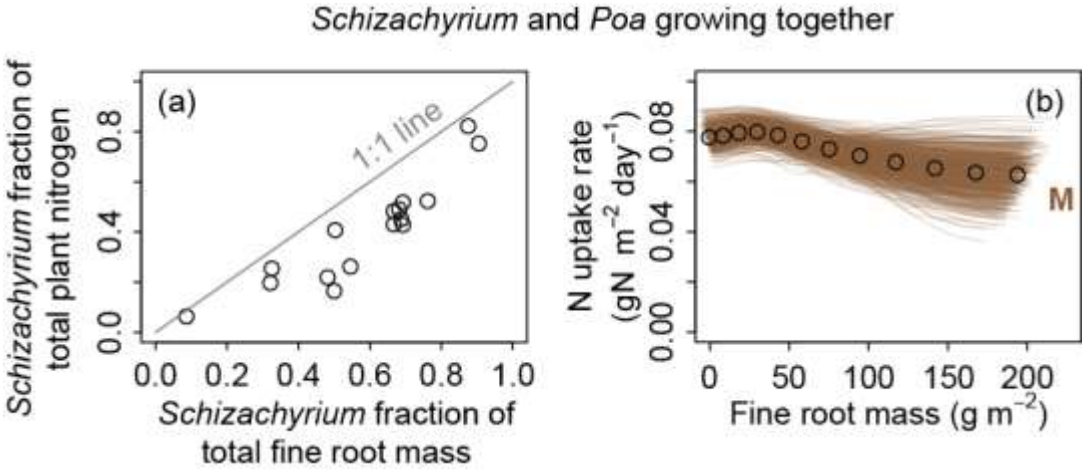

Figure 6. **Previously published pot experiments reanalyzed (exp. 4)**: individual plant nitrogen uptake rate versus fine-root mass in pot experiment studies. Data for Poorter et al. (1995) (left panels) and Trinder et al. (2012) (right panels) using sand culture or soil, respectively. Lines show 500 bootstrapped relationships per species per treatment. Bootstrap colors represent treatment: red = lower-N Hoaglands, blue = higher-N Hoaglands, and gray = low-fertility agricultural soil, with black symbols used for actual data (see Fig. 2). Notice the very different N uptake rate and fine-root mass scales between the two sets of data: small rectangle insets in (b) and (d) indicate the full scale displayed in (a) and (c). Most parsimonious fits by AICc: M = grand mean (Fig. 1a); L = zero-intercept linear (Fig. 1b); S = zero-intercept saturating (Fig. 1c) ; M/S = grand mean and zero-intercept saturating are equally parsimonious (i.e. ΔAICc $\leq$ 2). Because of the distinct decrease in the Trinder *et al.* (2012) data for fine-root mass greater than 90 g m^{-2}, we separately fit models to all the data ("all root") and to only data for fine-root mass less than 90 g m^{-2} ("root < 90").

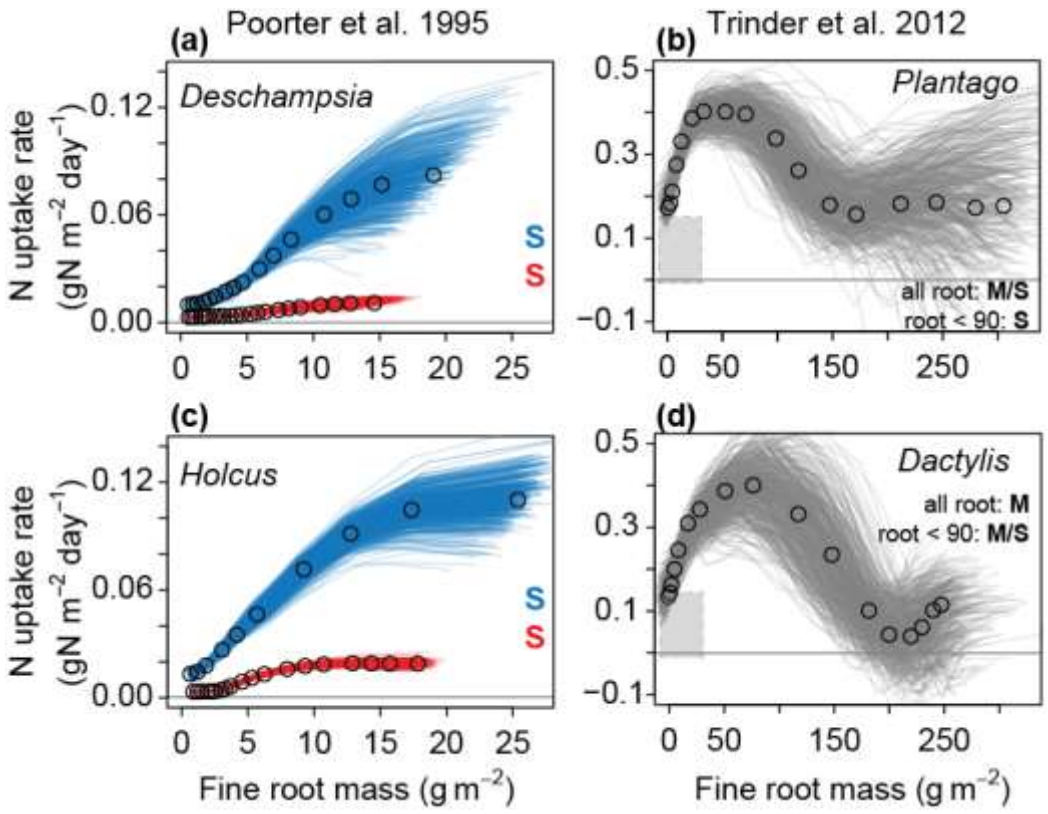

Figure 7. **Previously published field data reanalyzed (exp. 5)**: plant nitrogen uptake rate versus fine-root mass in forest field studies. Descriptions of each study are provided in the Methods and Table S4. We fit each set of data with three models corresponding to those commonly used in terrestrial biosphere models (see Fig. 1): M = grand mean (black, Fig. 1a); L = zero-intercept linear (purple, Fig. 1b); S = zero-intercept saturating (orange, Fig. 1c). The most parsimonious model is shown as solid & dark, and the other models are shown as dashed & transparent along with their number of ΔAIC points above the most parsimonious model. Open symbols represent ambient CO_2 plots; whereas closed symbols represent elevated CO_2 plots. Note that, unlike the microcosm or pot experiments, these field data do not have independent control (or even independent measures) of nitrogen availability. Thus, to the extent that nitrogen availability and fine-root mass are correlated, these figures confound the effects of nitrogen availability with fine-root mass.

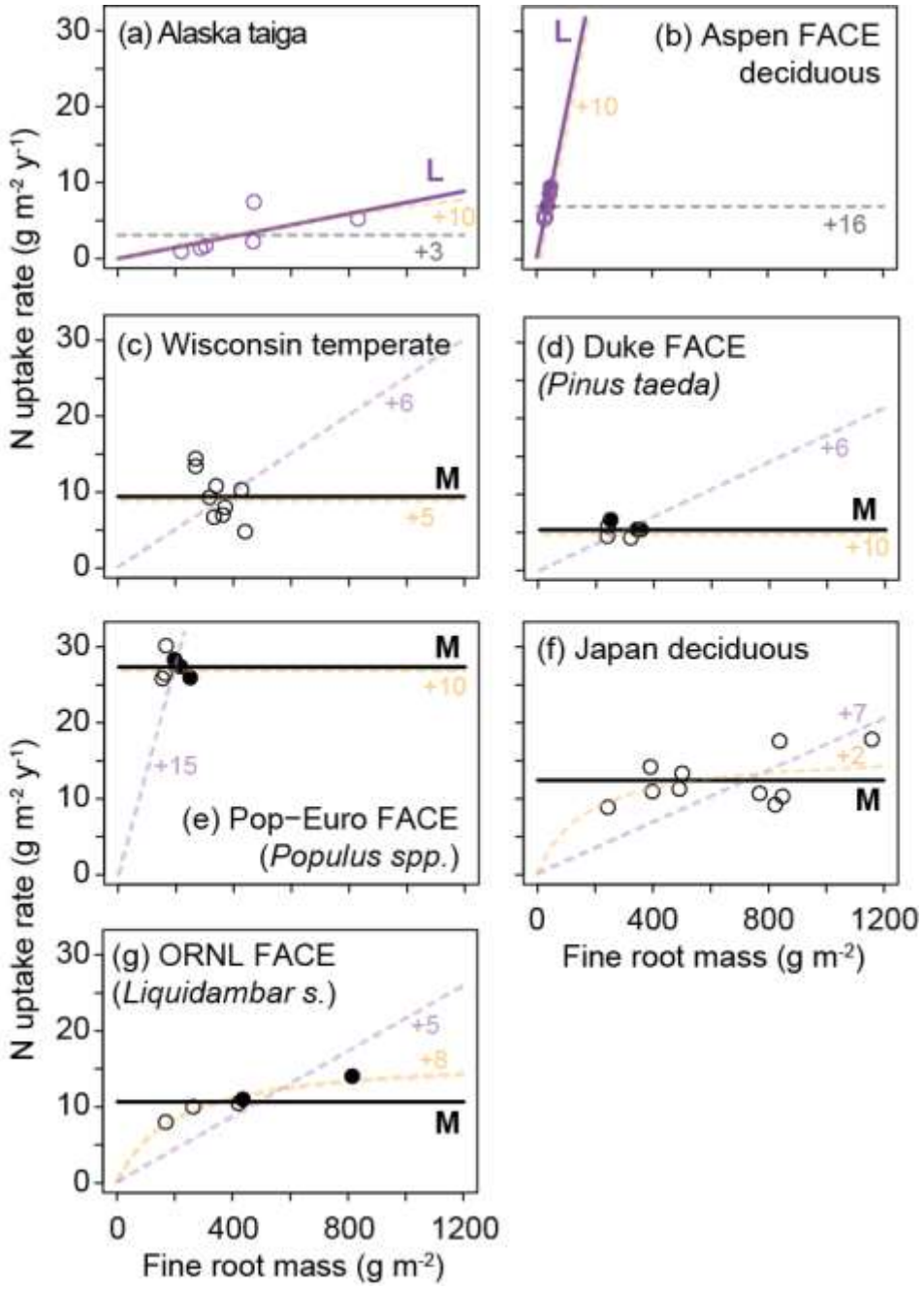
(a) Alaska taiga
L
+10
+3
(b) Aspen FACE
deciduous
L
+10
+16
(c) Wisconsin temperate
+6
M
+5
(d) Duke FACE
(Pinus taeda)
+6
M
+10
M
+10
+15
(e) Pop−Euro FACE
(Populus spp.)
(f) Japan deciduous
+7
+2
M
(g) ORNL FACE
(Liquidambar s.)
+5
+8
M
N uptake rate (g m-2 y-1)
Fine root mass (g m-2)
0
400
800
1200
10
20
30

851

Supplemental Online Material for: "How are nitrogen availability, fine-root mass, and nitrogen uptake related empirically? Implications for models and theory" by Dybzinski et al., Global Change Biology

SOM Figure S1. **Sand culture experiment (exp. 1):** The number of seedlings per microcosm at harvest for all three species. All values used in our analyses are on a per-microcosm basis, *not* on a per-seedling basis.

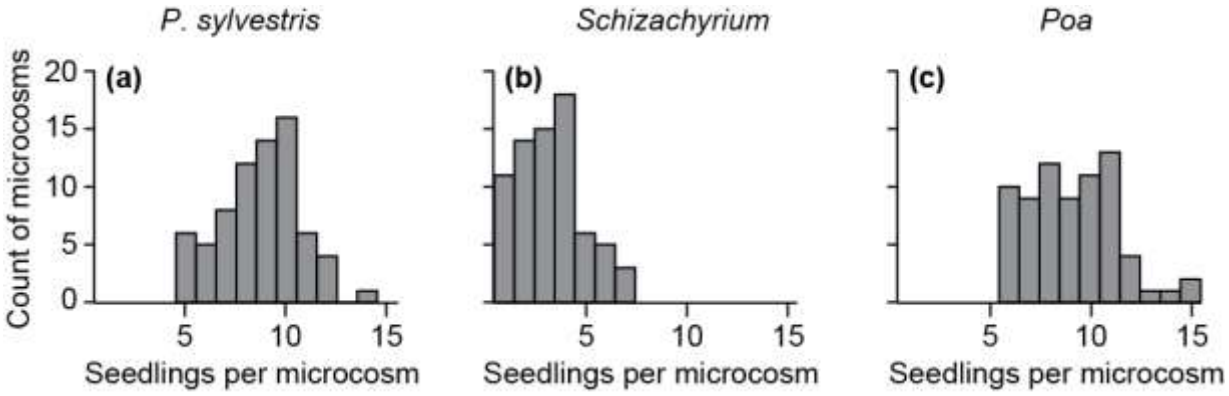

SOM Figure S2. **Sand culture experiment (exp. 1):** Total mass (a-c), shoot mass (d-f), root mass fraction (g-i), and fine-root mass (j-l) versus growing days at harvest. Colors represent nitrogen application rate: red = low (0.057 mgN d^{-1}); brown = medium (0.237 mgN d^{-1}); and blue = high (1.139 mgN d^{-1}). Lines represent spline fits. Species are separated by columns. Open circles represent individual data points.

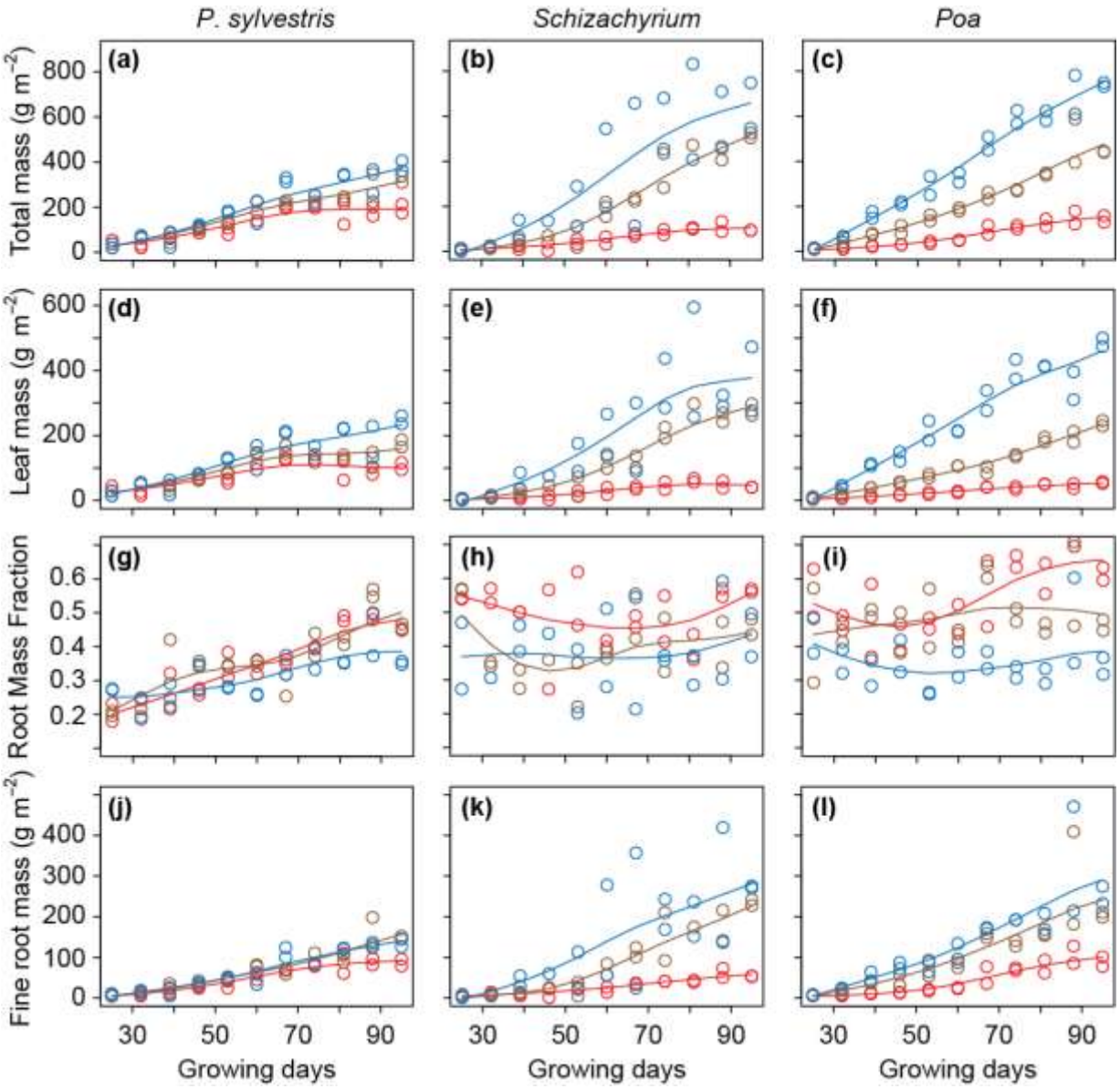

SOM Figure S3. **Sand culture experiment (exp. 1):** Shoot nitrogen concentration (a-c) and root nitrogen concentration (d-f) versus growing days at harvest; shoot nitrogen concentration versus shoot mass (g-i); and root nitrogen concentration versus root mass (j-l). Colors represent nitrogen application rate: red = low (0.057 mgN d^{-1}); brown = medium (0.237 mgN d^{-1}); and blue = high (1.139 mgN d^{-1}). Lines represent spline fits. Species are separated by columns. Open circles represent individual data points.

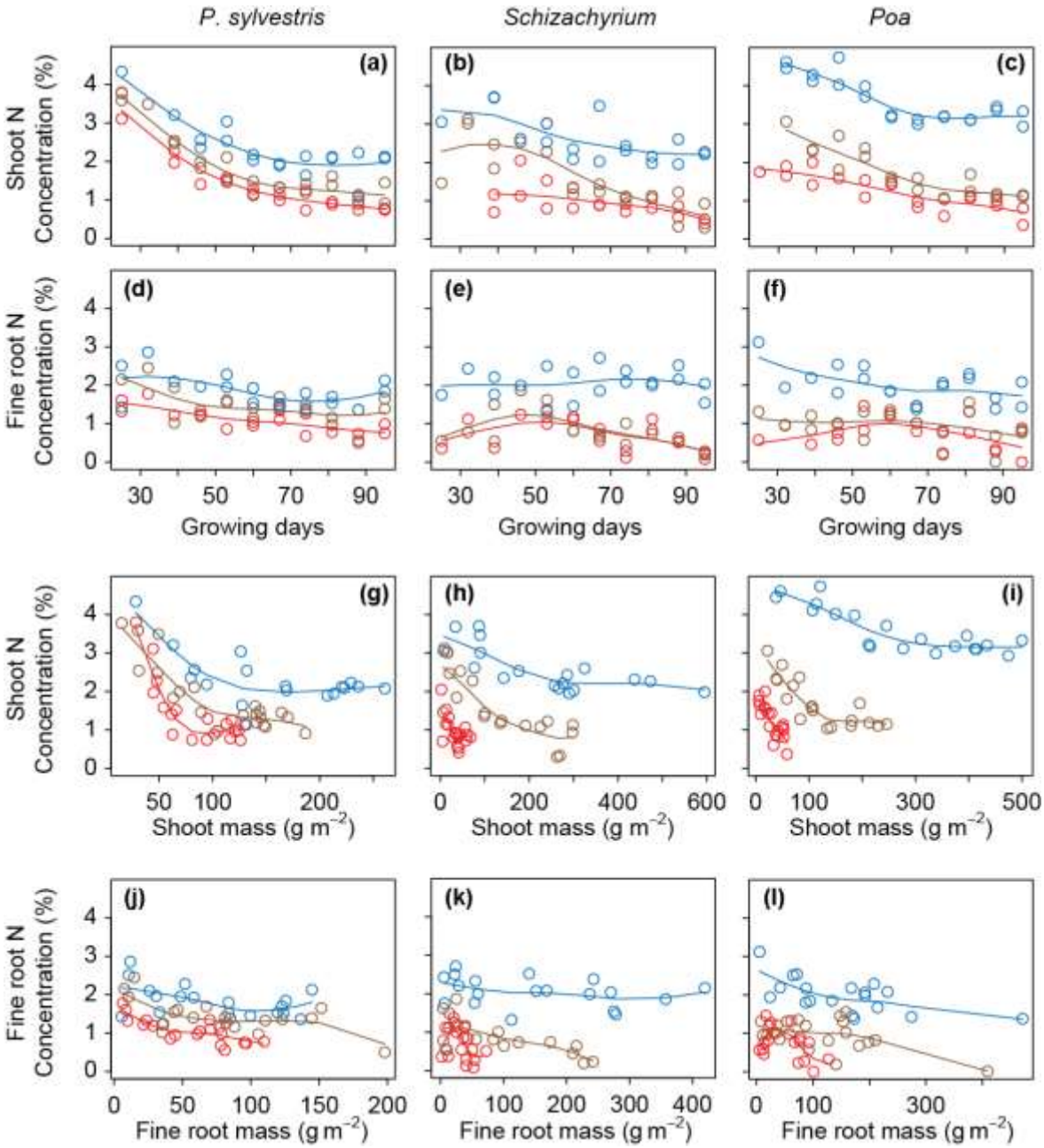

SOM Figure S4. **Sand culture experiment (exp. 1):** Total plant nitrogen uptake (calculated as total plant N minus nitrogen present in seeds) versus time for different nitrogen application rates: red = low (0.057 mgN d^{-1}); brown = medium (0.237 mgN d^{-1}); and blue = high (1.139 mgN d^{-1}). Note different y-axis ranges. Solid gray lines indicate the total amount of nitrogen that had been supplied as a function of growing days. We calculated the total nitrogen supplied to each microcosm by multiplying the nitrogen content of each fertigation by the number of fertigations at harvest, which was then added to the nitrogen that came with the substrate. Data points that rise above the gray supply lines reflect measurement error (and give an indication that values below the line also contain measurement error). Colored lines represent spline fits. Species are separated by columns. Open circles represent individual data points.

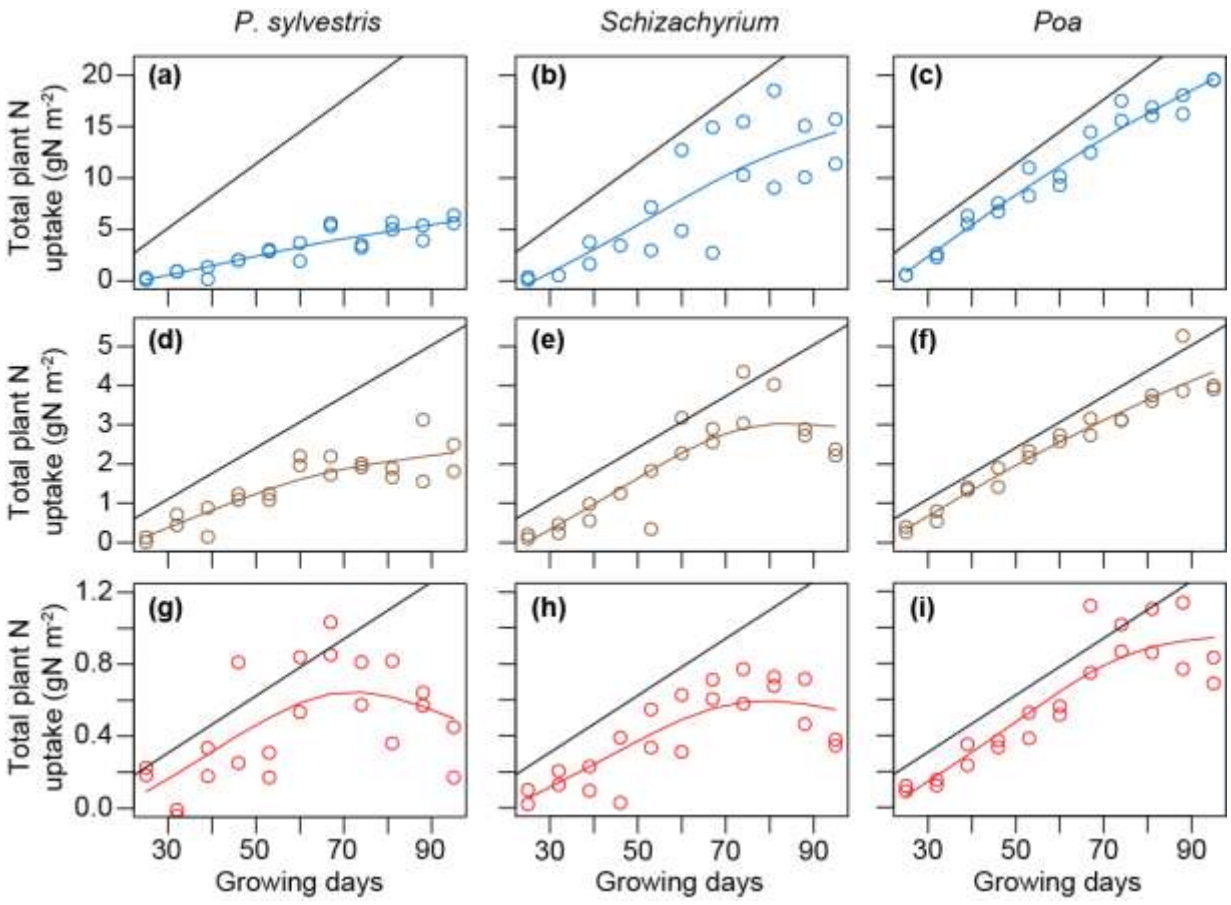

SOM Figure S5. **Sand culture experiment (exp. 1):** Fraction of supplied nitrogen that was taken up as a function of time (a-c) and as a function of root mass (d-f). We calculated the total nitrogen supplied to each microcosm by multiplying the nitrogen content of each fertigation by the number of fertigations at harvest, which was then added to the nitrogen that came with the substrate. Values that rise above unity reflect measurement error (and give an indication that values below unity also contain measurement error). Colors represent nitrogen application rate: red = low (0.057 mgN d^{-1}); brown = medium (0.237 mgN d^{-1}); and blue = high (1.139 mgN d^{-1}). Lines represent spline fits. Species are separated by columns. Open circles represent individual data points.

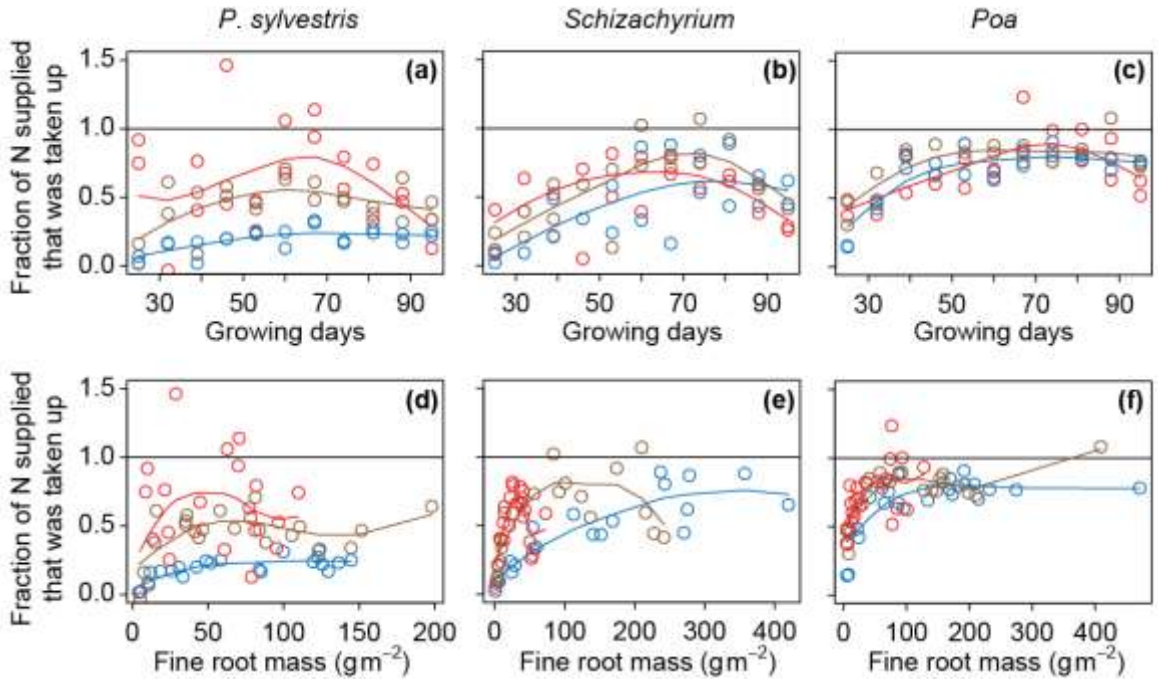

SOM Figure S6. **Sand culture experiment (exp. 1):** Average per seedling mass (total microcosm mass divided by the number of seedlings in the microcosm) versus growing days. Colors represent nitrogen application rate: red = low (0.057 mgN d^{-1}); brown = medium (0.237 mgN d^{-1}); and blue = high (1.139 mgN d^{-1}). Lines represent spline fits. Species are separated by columns. Open circles represent individual data points.

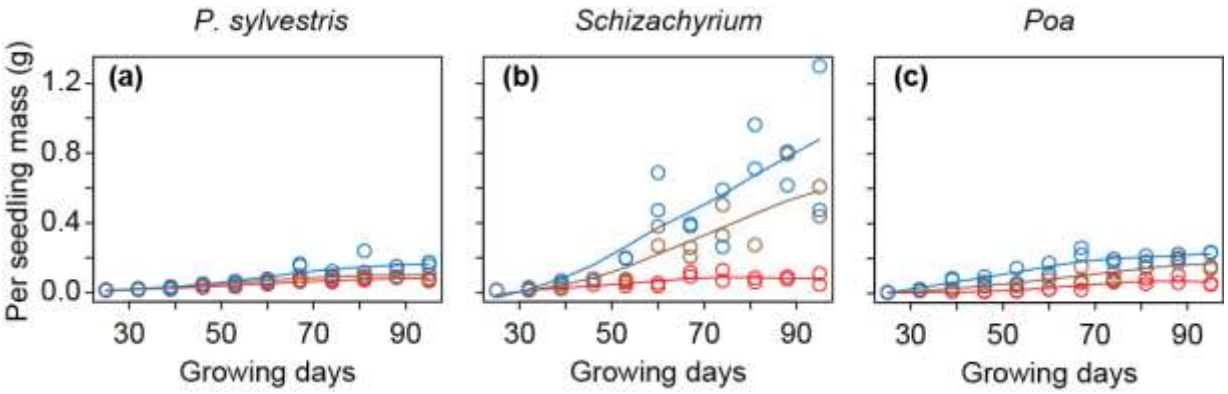

SOM Figure S7. **Soil experiment (exp. 2):** The number of seedlings per microcosm at harvest for angiosperms (a) and gymnosperms (b). Species are separated by columns. All values used in our analyses are on a per-microcosm basis, *not* on a per-seedling basis.

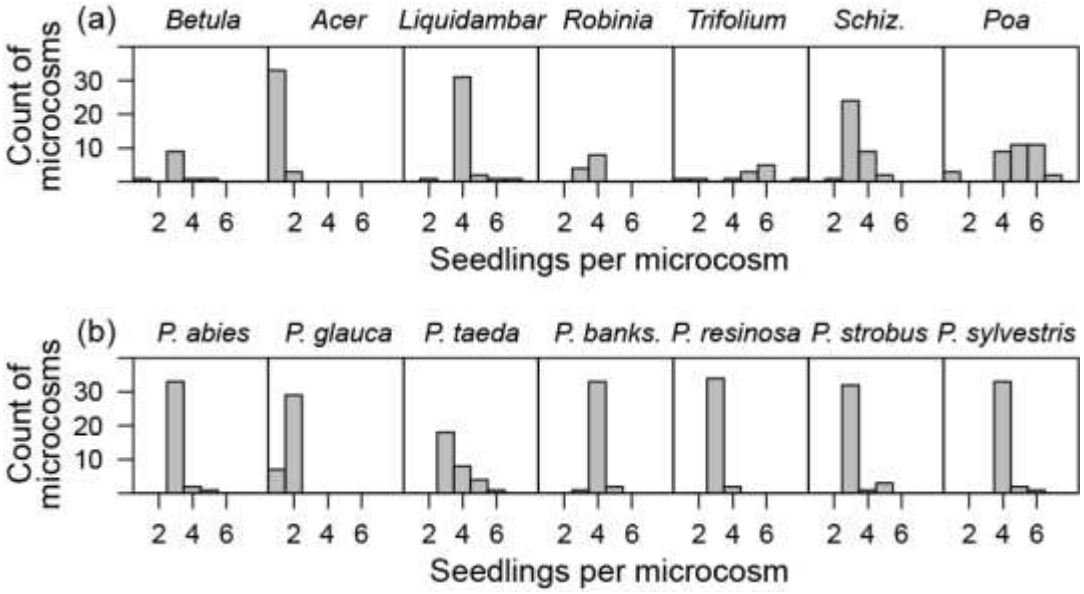

SOM Figure S8. **Soil experiment (exp. 2):** Leaf mass (g m^{-2}), stem mass (g m^{-2}), leaf mass fraction (LMF, leaf mass/total mass), fine-root mass fraction (fRMF, fine-root mass/total mass), and fine-root mass (g m^{-2}) versus growing days at harvest for angiosperms (a) and gymnosperms (b). Colors represent soil fertility (red = low; blue = high). Species are separated by columns. Open circles represent individual data points.

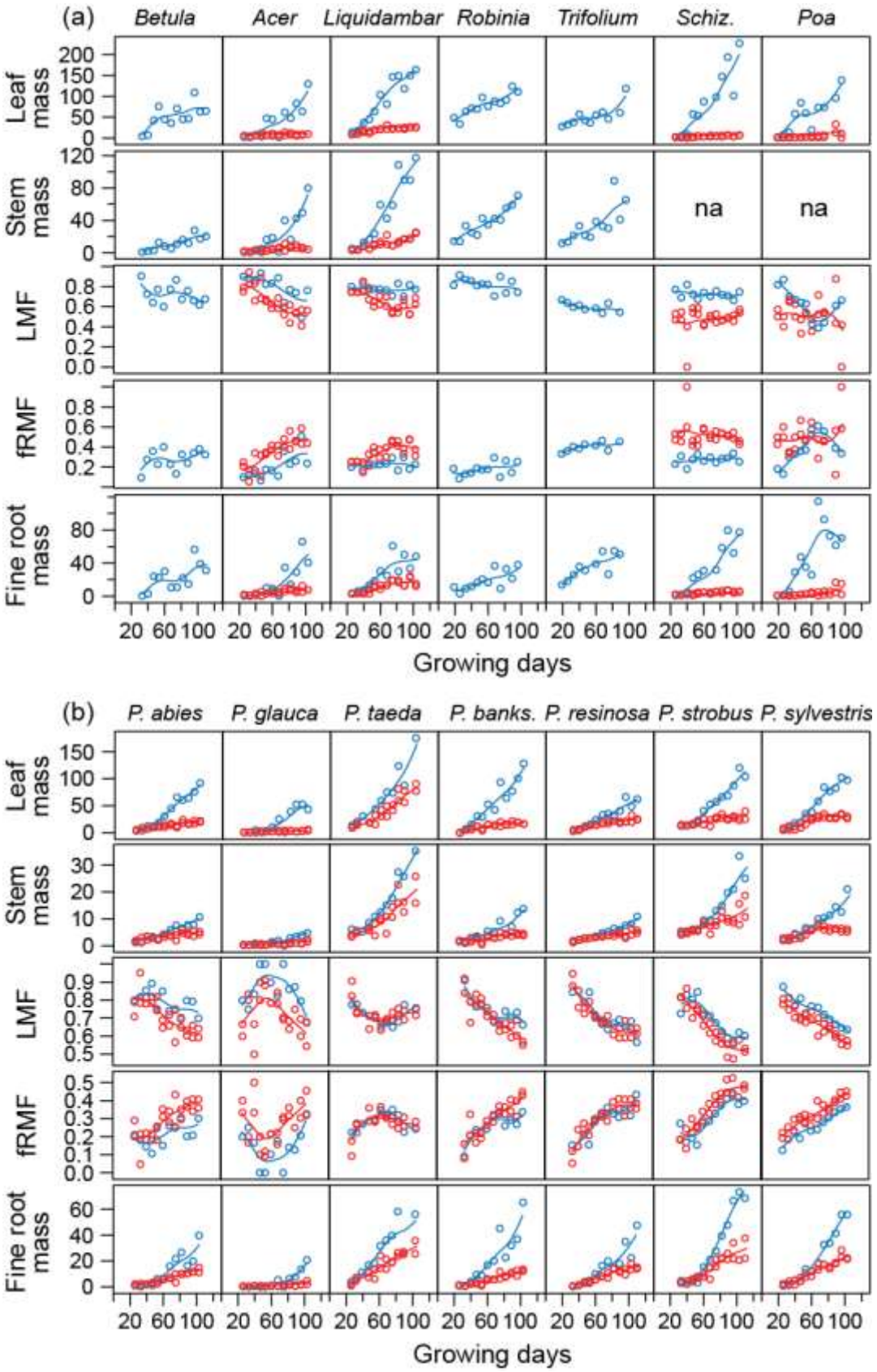
(a)
Betula
Acer
Liquidambar
Robinia
Trifolium
Schiz.
Poa
Leaf mass
Stem mass
LMF
fRMF
Fine root mass
na
na
Growing days
(b)
P. abies
P. glauca
P. taeda
P. banks.
P. resinosa
P. strobus
P. sylvestris
Leaf mass
Stem mass
LMF
fRMF
Fine root mass
Growing days

SOM Figure S9. **Soil experiment (exp. 2):** Leaf, stem, and fine-root nitrogen concentration versus growing days at harvest for angiosperms (a) and gymnosperms (b). Colors represent soil fertility (red = low; blue = high). Species are separated by columns. Open circles represent individual data points.

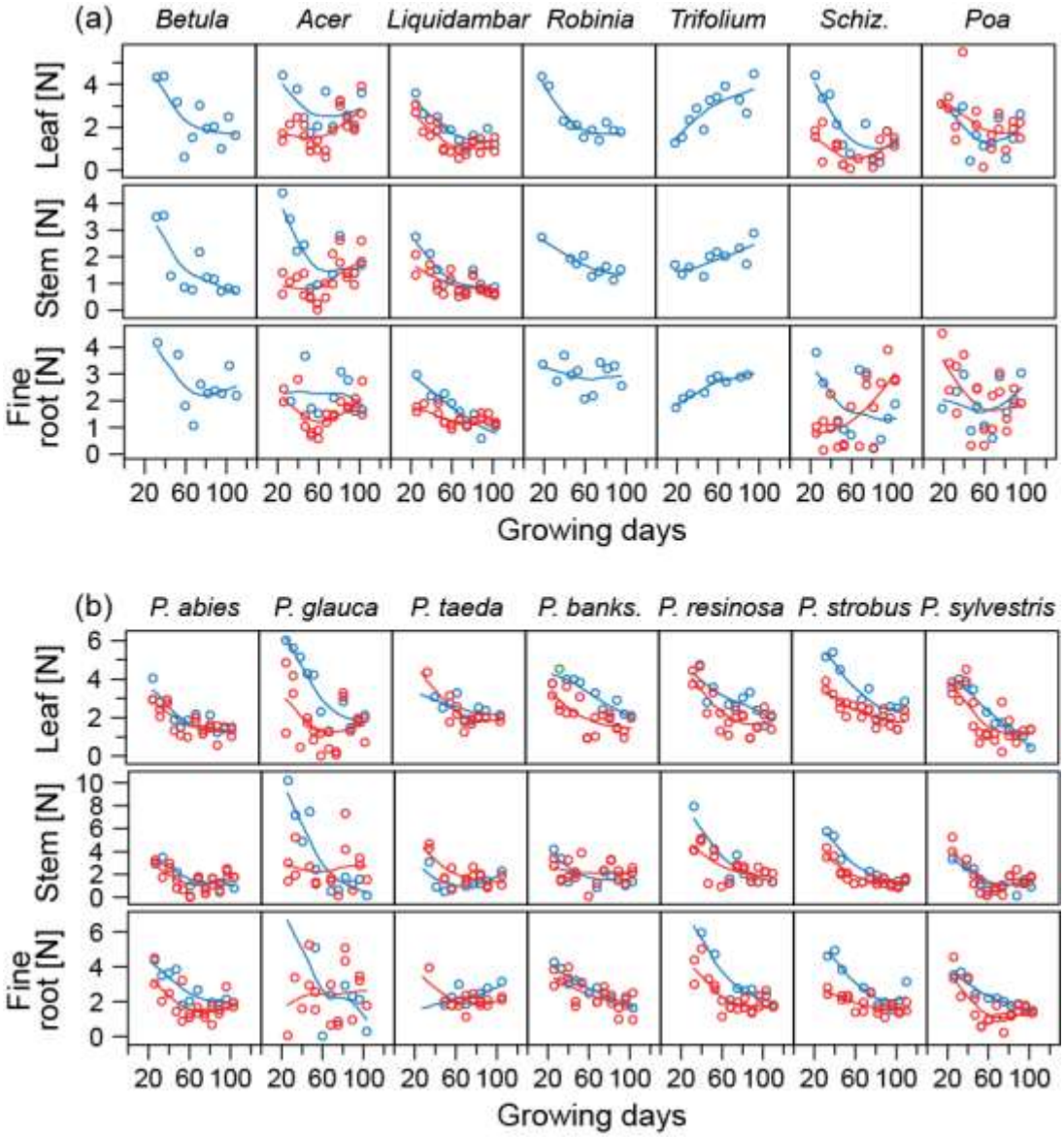

SOM Figure S10. **Soil experiment (exp. 2):** total plant nitrogen uptake (calculated as total plant N minus nitrogen present in seeds) versus growing days at harvest for angiosperms (a) and gymnosperms (b). Colors represent soil fertility (red = low; blue = high). Open circles represent individual data points.

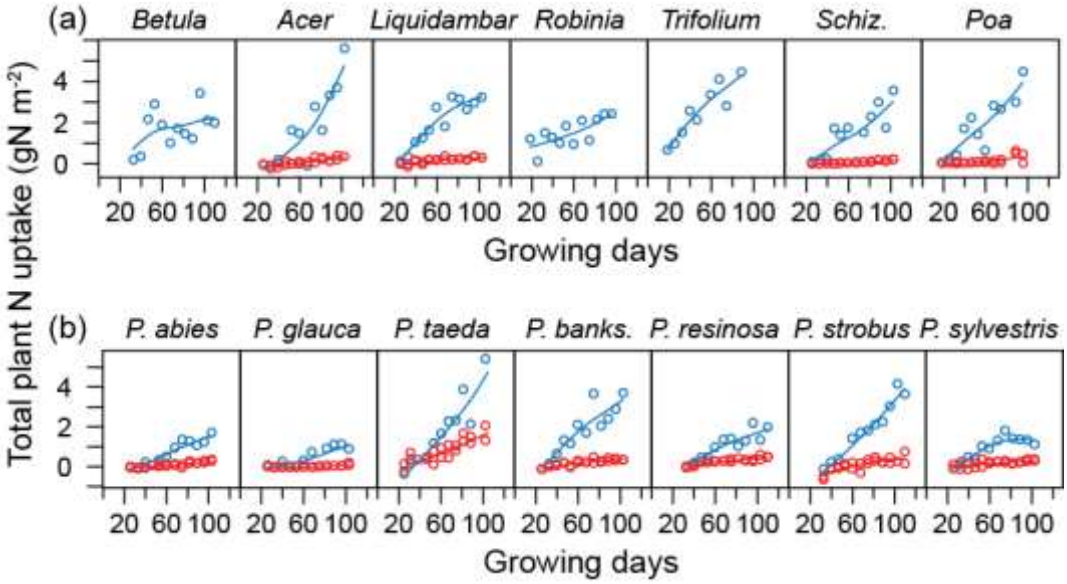

SOM Figure S11. **Sand culture two-species replacement series experiment (exp. 3):** The number of seedlings per microcosm at harvest for all four unique seeding densities and ratios, separated by columns (orange = *Schizachyrium*, blue = *Poa*). All values used in our analyses are on a per-microcosm basis, *not* on a per-seedling basis.

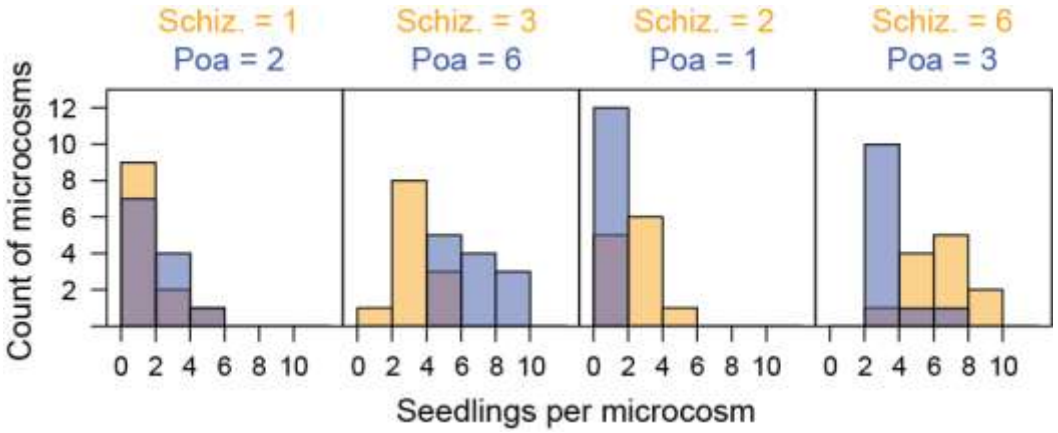

SOM Figure S12. **Sand culture two-species replacement series experiment (exp. 3):** Total mass (g m^{-2}), leaf mass (g m^{-2}), fine-root mass fraction (fRMF, fine-root mass/total mass), and fine-root mass (g m^{-2}) versus growing days at harvest for all four unique seeding densities and ratios, separated by columns (orange = *Schizachyrium*, blue = *Poa*, black = total). Open circles represent individual data points. Fine-root (and thus total) mass only shown separated to species for harvests 1 – 4 for which we were 100% certain fine roots were separated correctly to species.

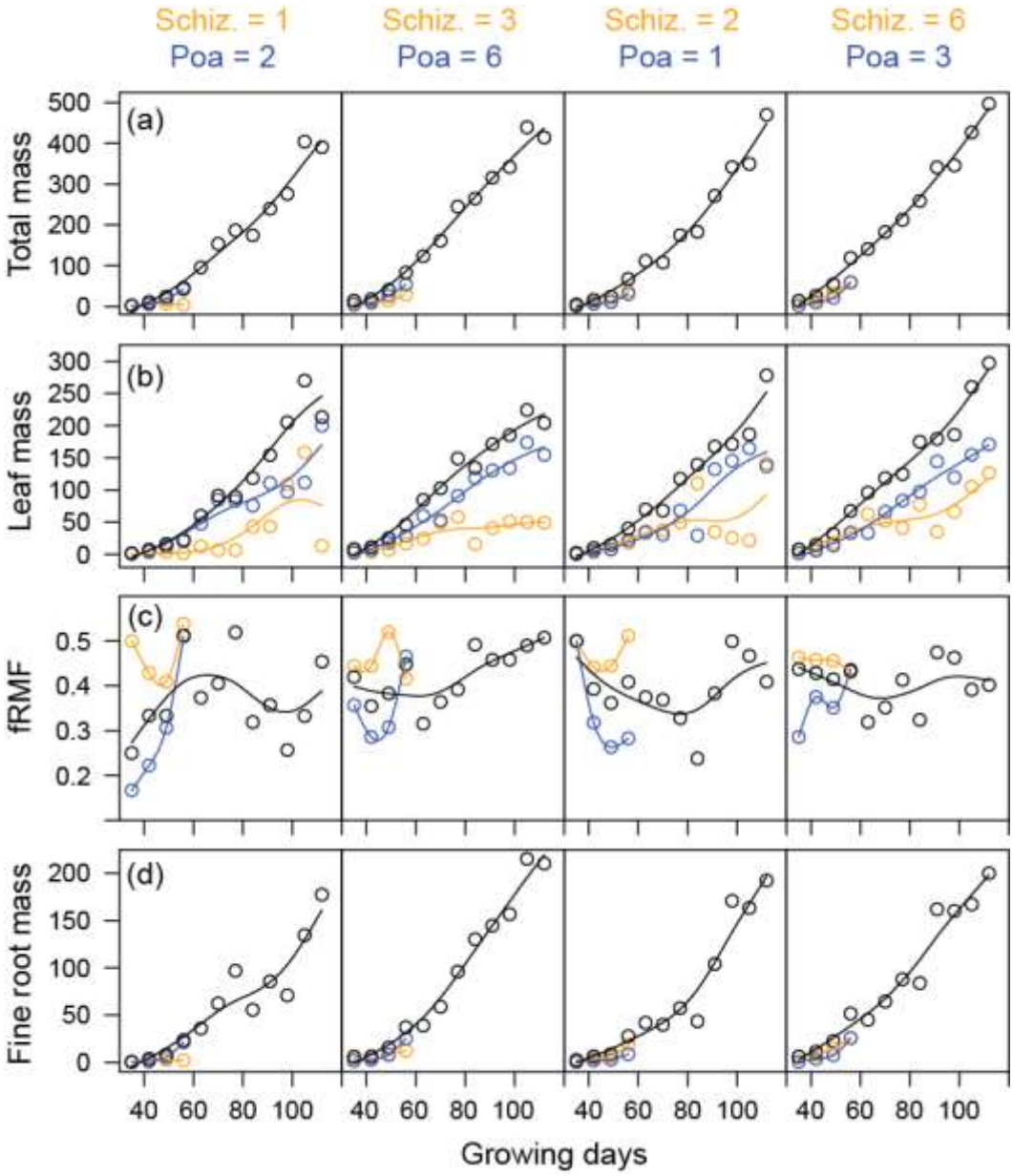

SOM Figure S13. **Sand culture two-species replacement series experiment (exp. 3):** Shoot (a) and fine-root (b) nitrogen concentration versus growing days at harvest for all four unique seeding densities and ratios, separated by columns (orange = *Schizachyrium*, blue = *Poa*). Open circles represent individual data points.

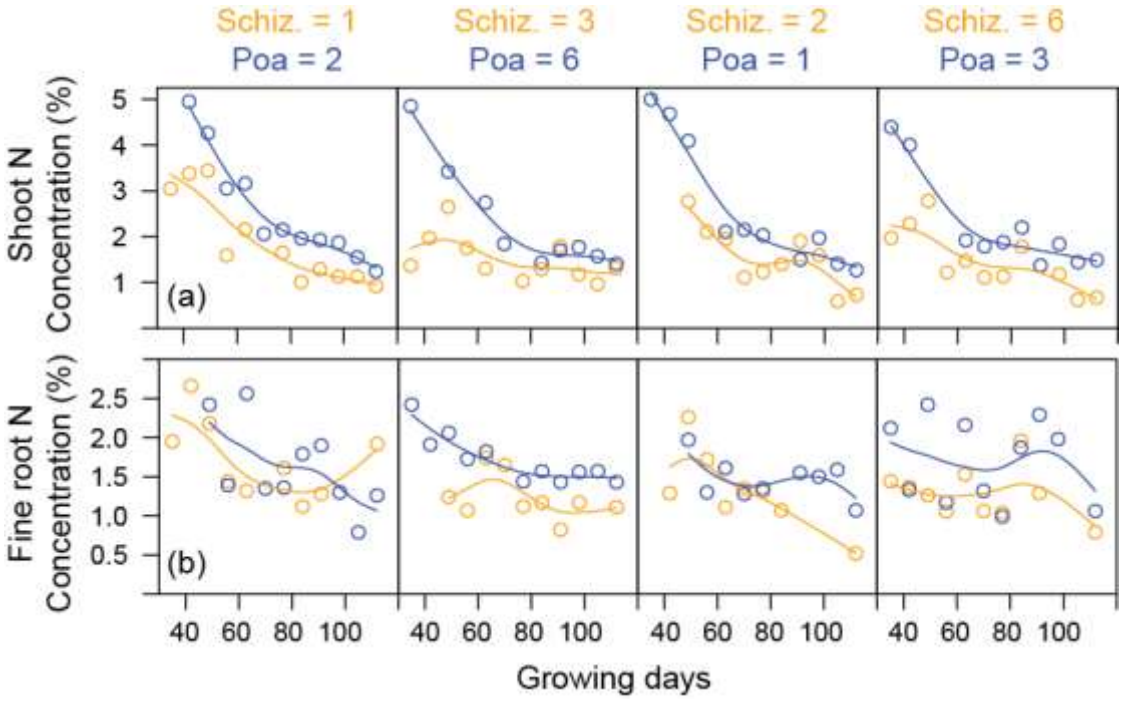

SOM Figure S14. **Sand culture two-species replacement series experiment (exp. 3):** Total plant nitrogen uptake (calculated as total plant N minus nitrogen present in seeds) versus growing days at harvest for all four unique seeding densities and ratios, separated by columns (orange = *Schizachyrium*, blue = *Poa*, black = total). Open circles represent individual data points.

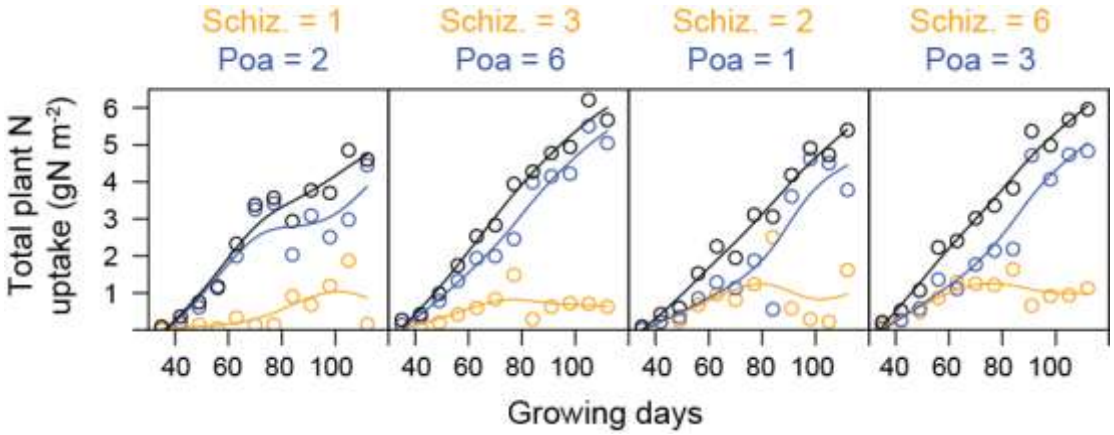

SOM Figure S15. **Sand culture two-species replacement series experiment (exp. 3):** The fraction of total (a-l) and shoot (m-x) nitrogen taken up by the population of *Schizachyrium* individuals versus their fraction of fine-root mass by harvest (H). We were certain of separation of fine roots to species for H1-4, reasonably confident for H5-8, and certain that some fine roots were misidentified for H9-12. The 1:1 line is shown for reference.

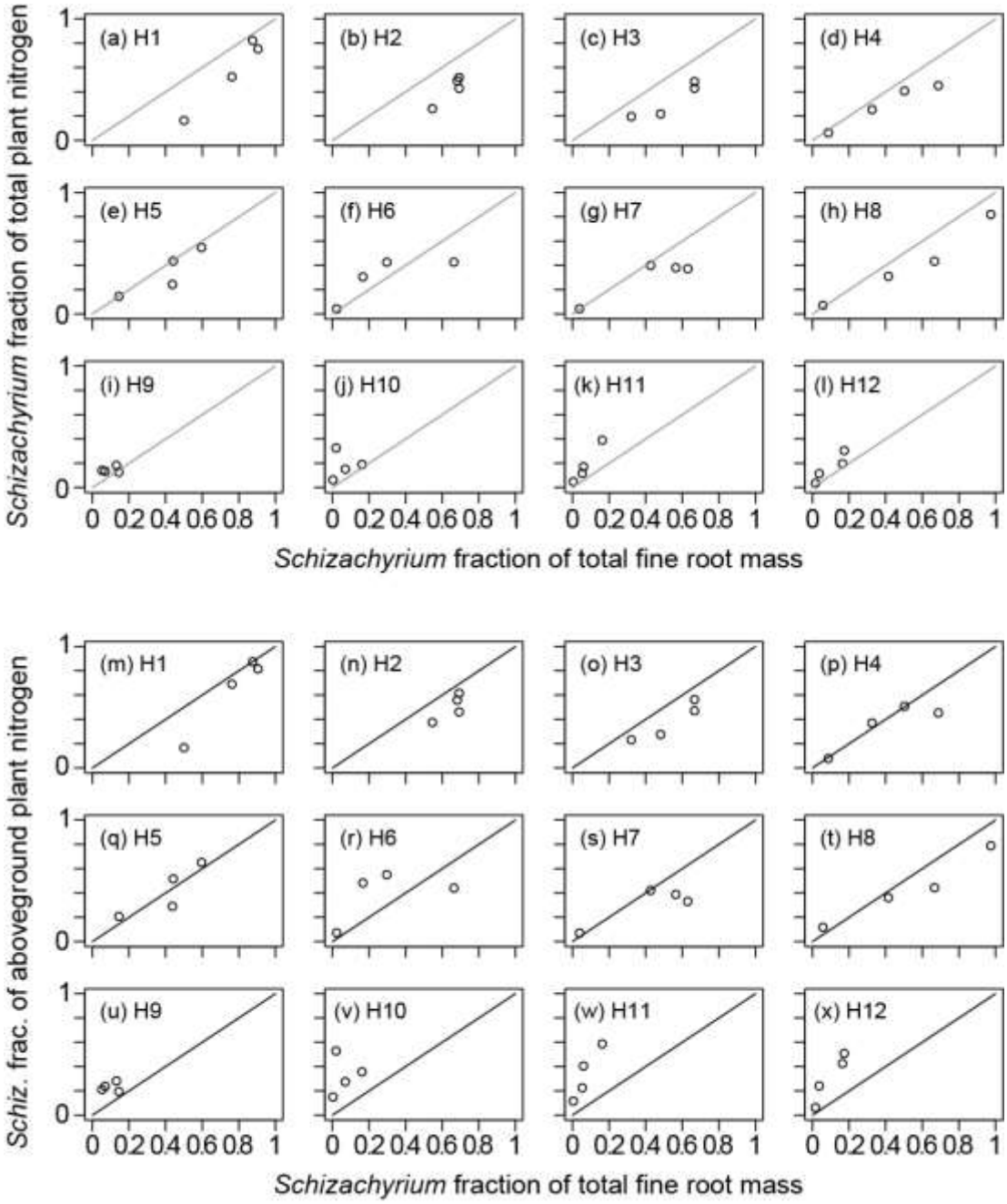

SOM Figure S16. **Previously published data reanalyzed (exp. 4):** total plant nitrogen and fine-root mass versus growing days in pot experiment studies. Data for Poorter *et al.* (1995) (left panels) and Trinder *et al.* (2012) (right panels) using sand culture or soil, respectively. Colors represent treatment: red = lower-N Hoaglands, blue = higher-N Hoaglands, and gray = low-fertility agricultural soil. Notice the very different scales between the two sets of data. Open circles represent individual data points.

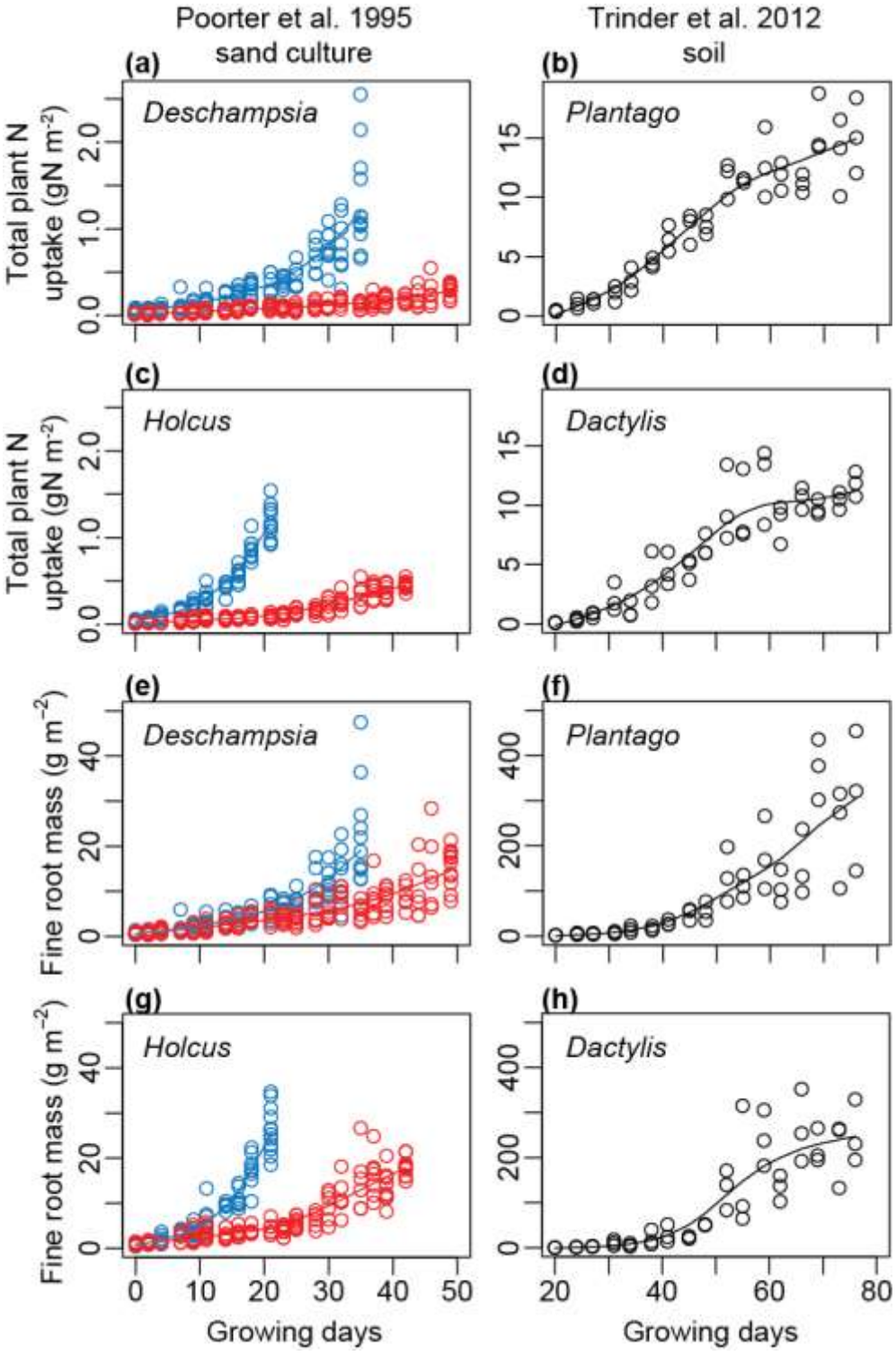
Poorter et al. 1995
sand culture
Trinder et al. 2012
soil
(a)
Deschampsia
(b)
Plantago
(c)
Holcus
(d)
Dactylis
(e)
Deschampsia
(f)
Plantago
(g)
Holcus
(h)
Dactylis
Total plant N uptake (gN m-2)
Fine root mass (g m-2)
Growing days
0.0
1.0
2.0
0
5
10
15
0
20
40
200
400
0
10
20
30
40
50
60
80

958

959

SOM Figure S17. **A separate sand culture microcosm experiment with different planting densities**: plant community nitrogen uptake rate versus fine-root mass. The experiment, which is not described elsewhere in the main text except as a discussion point, was conducted between March and July of 2017 using the same facilities and lighting described above for our sand culture experiment. Average low and high temperatures were 20C and 30C, and the average daily light integral over the duration of the experiment was 10.9M m^{-2} d^{-1}. We used *Schizachyrium scoparium*, a C4 grass, and *Poa pratensis*, a C3 grass (Sheffield's Seed Company, Locke, New York, USA). Except for the density treatment and replicates indicated below, all other aspects of the experiment were identical to our sand-culture experiment described above. We used one replicate per species per each of three seedling densities (1 (open circles), 3 (triangles), or 9 (stars) per cup), per each of three fertility levels, and per each of 12 weekly harvests. In all, each species had 3 density levels, 3 fertility levels, 12 harvests, and 1 replicate for 108 microcosms per species and 216 microcosms total. Lines show 500 bootstrapped relationships per species per nitrogen level. Colors represent nitrogen application rate: red = low (0.057 mgN d^{-1}); brown = medium (0.237 mgN d^{-1}); and blue = high (1.139 mgN d^{-1}). Most parsimonious fits by AICc: M = grand mean (Fig. 1a); L = zero-intercept linear (Fig. 1b); S = zero-intercept saturating (Fig. 1c).

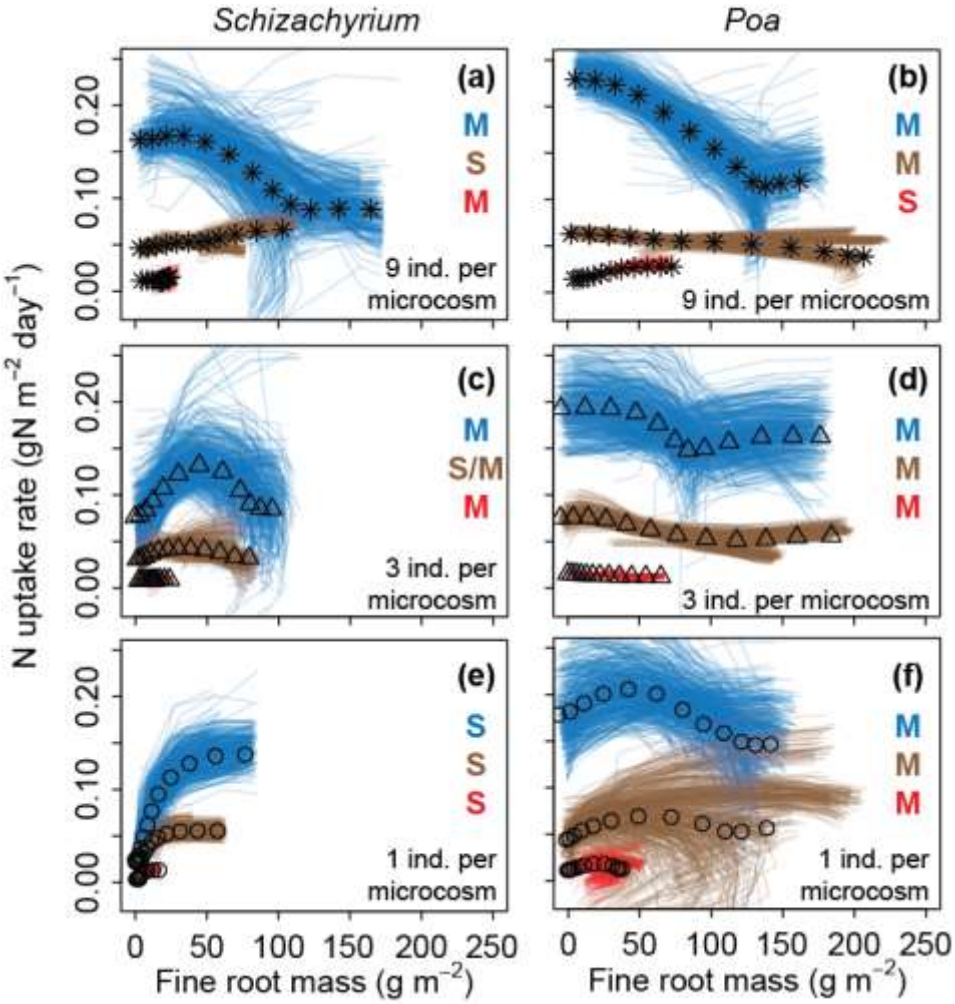
Schizachyrium
Poa
(a)
M
S
M
9 ind. per microcosm
(b)
M
M
S
9 ind. per microcosm
(c)
M
S/M
M
3 ind. per microcosm
(d)
M
M
M
3 ind. per microcosm
(e)
S
S
S
1 ind. per microcosm
(f)
M
M
M
1 ind. per microcosm
N uptake rate (gN m^{-2} day^{-1})
0.00
0.10
0.20
0 50 100 150 200 250
Fine root mass (g m^{-2})

975

976

SOM Figure S18. **A separate sand culture microcosm experiment with different planting densities**: plant community nitrogen uptake rate versus fine-root mass. The experiment, which is not described elsewhere in the main text except as a discussion point, was conducted in the spring of 2017 following the methods of our sand culture experiment, except that there was only one replicate per species, harvest, nitrogen level, and density. See legend for Fig. S17 for more details. Apart from that, the main difference between this separate study and the sand culture study presented in the main text is that we manipulated the density of individuals per microcosm to 1 (circles), 3 (triangles), or 9 (stars). The data are presented here linked by harvest day: each color represents a different harvest day, approximately one week apart, with the earliest harvests to the left of each panel and the later harvests to the right of each panel. Notice that panels a, b, c, & e show an increasing relationship between plant community nitrogen uptake rate and fine-root mass for the earliest harvests, but that no systematic relationship exists for the later harvests. In other words, for the later harvests, differences in root mass attributable to planting density suggest the same results that we obtained in the other experiments, where differences in root mass were attributable to ontogeny: no relationship between plant community nitrogen uptake rate and fine-root mass. Notice also the differences in scale for each panel. Together, these demonstrate that ontogeny's effect was minimal, swamped by differences in nitrogen availability, and gone after several harvests. These are an alternative way of viewing the data presented in Fig. S17.

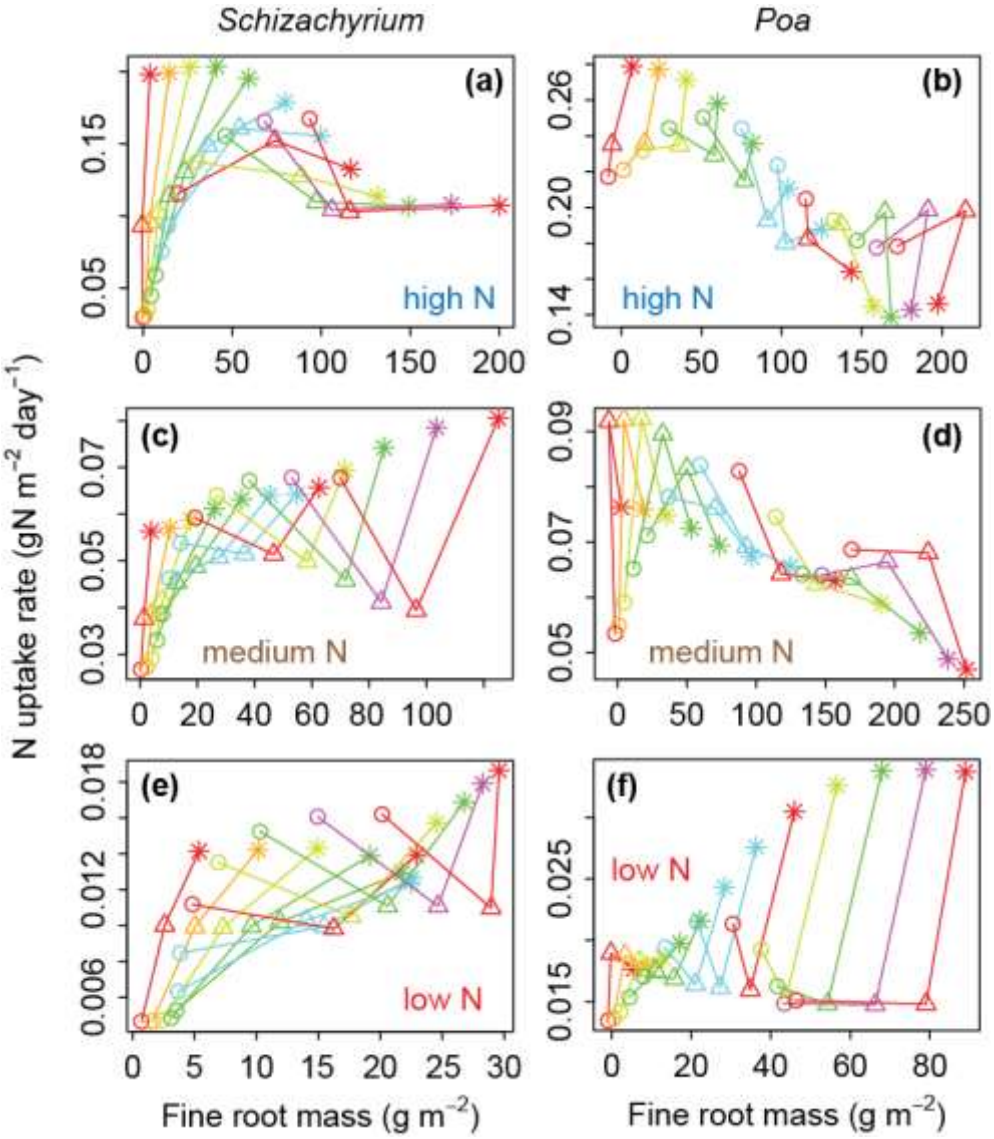
Schizachyrium
Poa
(a)
(b)
(c)
(d)
(e)
(f)
high N
high N
medium N
medium N
low N
low N
N uptake rate (gN m^{-2} day^{-1})
Fine root mass (g m^{-2})
Fine root mass (g m^{-2})

994

SOM Table S1. Functional forms of plant nitrogen uptake rate for coupled-CN terrestrial biosphere models. "Equation(s)" refers to the equation number in cited paper that describes nitrogen uptake rate.

Model	**Source**	**Equation(s)**	**Type**
GDAY	Comins and McMurtrie (1993)	9	No fine-root dependence
SDGVM	Woodward *et al.* (1995)	31	No fine-root dependence
CABLE	Wang *et al.* (2010)	6	No fine-root dependence
CLM4.5	Oleson *et al.* (2013)	13.13 – 13.17	No fine-root dependence
TEM	Raich *et al.* (1991)	1.16	Linear fine-root dependence
EALCO	Wang *et al.* (2001)	16	Linear fine-root dependence
ISAM	Yang *et al.* (2009)	12a	Linear fine-root dependence
O-CN	Zaehle and Friend (2010)	8	Linear fine-root dependence
LM3V	Gerber *et al.* (2010)	10	Linear fine-root dependence
CLASS-CTEM^{N+}	Huang *et al.* (2011)	A6, A7a, A7b	Linear fine-root dependence
LPJ-GUESS	Smith *et al.* (2014)	C14	Linear fine-root dependence
TECO-CN*	E. Weng, personal communication	Na	Saturating fine-root dep.

* TECO-CN, was only published as part of a model inter-comparison study (Zaehle *et al.*, 2014)

SOM Table S2. Nitrogen content of seeds used in our microcosm experiments (exps. 1 – 3). We counted 100 seeds per species, determined their mass, and divided by 100 to determine the per-seed mass. We used all 100 seeds per species to determine the nitrogen fraction, which we then multiplied by per-seed mass to determine nitrogen per seed.

Species	Nitrogen per seed (mg)
Acer rubrum	0.6662
Betula papyrifera	0.0564
Liquidambar styraciflua	0.3315
Picea abies	0.3641
Picea glauca	0.1591
Pinus banksiana	0.2206
Pinus resinosa	0.4102
Pinus strobus	1.0864
Pinus sylvestris	0.4178
Pinus taeda	0.7228
Poa pratensis	0.0065
Robinia pseudoacacia	1.6051
Schizachyrium scoparium	0.0271
Trifolium pratense	0.1090

SOM Table S3. Soil experiment (exp. 2): evidence that the two lowest fertility treatments did not produce appreciably different biomass or plant nitrogen and thus could be merged into a single "low fertility" soil treatment with greater replication. All response data were log transformed to meet assumptions of normality and homoscedasticity. Analyses shown below exclude the high fertility treatments (100% soil). Note, if high fertility treatments *are* included in the analyses, *all* soil fertility effects become highly significant ($P < 2 \times 10^{-16}$).

Root mass

	Df	Sum Sq	Mean Sq	F value	Pr(>F)	
Time	1	172.20	172.20	657.418	<2e-16	***
Species	10	123.02	12.30	46.965	<2e-16	***
Soil fertility	1	0.87	0.87	3.307	0.0702	.
Residuals	245	64.18	0.26			

Stem & taproot mass

	Df	Sum Sq	Mean Sq	F value	Pr(>F)	
Time	1	49.98	49.98	465.024	<2e-16	***
Species	8	124.98	15.62	145.347	<2e-16	***
Soil fertility	1	0.19	0.19	1.798	0.181	
Residuals	199	21.39	0.11			

Leaf mass

	Df	Sum Sq	Mean Sq	F value	Pr(>F)	
Time	1	87.88	87.88	647.784	<2e-16	***
Species	10	154.29	15.43	113.736	<2e-16	***
Soil fertility	1	0.33	0.33	2.428	0.12	
Residuals	239	32.42	0.14			

Total plant mass

	Df	Sum Sq	Mean Sq	F value	Pr(>F)	
Time	1	106.30	106.30	794.614	<2e-16	***
Species	10	132.07	13.21	98.726	<2e-16	***
Soil fertility	1	0.63	0.63	4.737	0.0305	*
Residuals	239	31.97	0.13			

Plant nitrogen

	Df	Sum Sq	Mean Sq	F value	Pr(>F)	
Time	1	141.52	141.52	195.576	<2e-16	***
Species	10	106.15	10.62	14.670	<2e-16	***
Soil fertility	1	2.83	2.83	3.918	0.0492	*
Residuals	195	141.10	0.72			

SOM Table S4. Details on previously published field data reanalyzed (exp. 5). All studies used soil cores to measure fine-root mass. References for each study are in the main text. BrN(t) = this year's branch nitrogen increment. BoN(t) = this year's bole nitrogen increment. CRN(t) = this year's coarse root nitrogen increment. LN(t) = this year's leaf mass. LN(t-1) = last year's litter. LNr(t-1) = last year's resorbed leaf nitrogen. FRN(t) = this year's fine-root nitrogen increment. NminRate = nitrogen mineralization rate. NDepRate = nitrogen deposition rate. NLchRate = nitrogen leaching rate. NFixRate = nitrogen fixation rate. DBH = stem diameter at breast height.

Study	Pop-Euro FACE	Duke FACE	Wisconsin temperate	Aspen FACE	Alaska taiga	ORNL FACE	Japan deciduous
N uptake rate equation	BrN(t) +BoN(t) +CRN(t) +LN(t) –LNr(t-1) +FRN(t)	BrN(t) +BoN(t) +CRN(t) +LN(t) –LNr(t-1) +FRN(t)	NminRate +NDepRate –NLchRate	BrN(t) +BoN(t) +CRN(t) +LN(t) –LNr(t-1) +FRN(t)	NminRate +NDepRate +NFixRate	BrN(t) +BoN(t) +CRN(t) +LN(t) –LNr(t-1) +FRN(t)	BrN(t) +BoN(t) +CRN(t) +LN(t-1) +FRN(t)
BrN(t), BoN(t), &CRN(t)	destructive harvest	allometric w/ DBH + [N]	-	destructive harvest	-	allometric w/ DBH + [N]	allometric w/ DBH + [N]
LN(t) & LNr(t-1)	litter baskets	litter baskets	-	litter baskets	-	litter baskets	litter baskets, just used N content of litter
FRN(t)	ingrowth cores + [N]	minirhizotrons + [N]	-	literature data + allometric w/ DBH	-	minirhizotrons + [N]	ingrowth cores + [N]
NminRate	-	-	buried bags	-	buried bags	-	-
NDepRate	-	-	nearby weather station	-	assumed constant 0.2gN m^{-2} yr^{-1}	-	-

NLchRate	-	-	lysimeters	-	-	-	-
NFixRate	-	-	-	-	estimated from chronosequence	-	-

1056

1057

SOM Table S5. Goodness of fit (R^2) for all splines, calculated using the standard definition: $1 - \sum \varepsilon^2 / \sum (y - \bar{y})^2$, where ε is the vector of residuals from the spline, y is the vector of the response variable, and $\bar{y}$ is the average of the response variable.

Relationship	Figure	Panel	Line	R^2
Mass vs. time	S2	a	High	0.88
Mass vs. time	S2	a	Low	0.86
Mass vs. time	S2	a	Medium	0.92
Mass vs. time	S2	b	High	0.72
Mass vs. time	S2	b	Low	0.88
Mass vs. time	S2	b	Medium	0.95
Mass vs. time	S2	c	High	0.97
Mass vs. time	S2	c	Low	0.92
Mass vs. time	S2	c	Medium	0.94
Mass vs. time	S2	d	High	0.83
Mass vs. time	S2	d	Low	0.77
Mass vs. time	S2	d	Medium	0.87
Mass vs. time	S2	e	High	0.71
Mass vs. time	S2	e	Low	0.82
Mass vs. time	S2	e	Medium	0.94
RMF vs. time	S2	f	High	0.94
RMF vs. time	S2	f	Low	0.93
RMF vs. time	S2	f	Medium	0.97
RMF vs. time	S2	g	High	0.61
RMF vs. time	S2	g	Low	0.89
RMF vs. time	S2	g	Medium	0.75
RMF vs. time	S2	h	High	0.06
RMF vs. time	S2	h	Low	0.24
RMF vs. time	S2	h	Medium	0.48
RMF vs. time	S2	i	High	0.19
RMF vs. time	S2	i	Low	0.60
RMF vs. time	S2	i	Medium	0.12
Mass vs. time	S2	j	High	0.92
Mass vs. time	S2	j	Low	0.91
Mass vs. time	S2	j	Medium	0.88
Mass vs. time	S2	k	High	0.56
Mass vs. time	S2	k	Low	0.87
Mass vs. time	S2	k	Medium	0.90
Mass vs. time	S2	l	High	0.78

Relationship	Figure	Panel	Line	R^2
Mass vs. time	S2	l	Low	0.88
Mass vs. time	S2	l	Medium	0.75
[N] vs. time	S3	a	High	0.80
[N] vs. time	S3	a	Low	0.95
[N] vs. time	S3	a	Medium	0.93
[N] vs. time	S3	b	High	0.53
[N] vs. time	S3	b	Low	0.56
[N] vs. time	S3	b	Medium	0.71
[N] vs. time	S3	c	High	0.86
[N] vs. time	S3	c	Low	0.76
[N] vs. time	S3	c	Medium	0.83
[N] vs. time	S3	d	High	0.44
[N] vs. time	S3	d	Low	0.63
[N] vs. time	S3	d	Medium	0.45
[N] vs. time	S3	e	High	0.09
[N] vs. time	S3	e	Low	0.46
[N] vs. time	S3	e	Medium	0.58
[N] vs. time	S3	f	High	0.42
[N] vs. time	S3	f	Low	0.36
[N] vs. time	S3	f	Medium	0.17
[N] vs. mass	S3	g	High	0.64
[N] vs. mass	S3	g	Low	0.92
[N] vs. mass	S3	g	Medium	0.72
[N] vs. mass	S3	h	High	0.75
[N] vs. mass	S3	h	Low	0.32
[N] vs. mass	S3	h	Medium	0.71
[N] vs. mass	S3	i	High	0.82
[N] vs. mass	S3	i	Low	0.65
[N] vs. mass	S3	i	Medium	0.83
[N] vs. mass	S3	j	High	0.34
[N] vs. mass	S3	j	Low	0.67
[N] vs. mass	S3	j	Medium	0.59
[N] vs. mass	S3	k	High	0.20
[N] vs. mass	S3	k	Low	0.49
[N] vs. mass	S3	k	Medium	0.45
[N] vs. mass	S3	l	High	0.48
[N] vs. mass	S3	l	Low	0.50
[N] vs. mass	S3	l	Medium	0.36
Total N vs. time	S4	a	High	0.85

Relationship	Figure	Panel	Line	R^2
Total N vs. time	S4	b	High	0.70
Total N vs. time	S4	c	High	0.97
Total N vs. time	S4	d	Medium	0.80
Total N vs. time	S4	e	Medium	0.85
Total N vs. time	S4	f	Medium	0.94
Total N vs. time	S4	g	Low	0.58
Total N vs. time	S4	h	Low	0.79
Total N vs. time	S4	i	Low	0.88
Frac N vs. time	S5	a	High	0.52
Frac N vs. time	S5	a	Low	0.26
Frac N vs. time	S5	a	Medium	0.42
Frac N vs. time	S5	b	High	0.75
Frac N vs. time	S5	b	Low	0.62
Frac N vs. time	S5	b	Medium	0.67
Frac N vs. time	S5	c	High	0.48
Frac N vs. time	S5	c	Low	0.58
Frac N vs. time	S5	c	Medium	0.65
Frac N vs. time	S5	d	High	0.69
Frac N vs. time	S5	d	Low	0.18
Frac N vs. time	S5	d	Medium	0.54
Frac N vs. time	S5	e	High	0.67
Frac N vs. time	S5	e	Low	0.47
Frac N vs. time	S5	e	Medium	0.75
Frac N vs. time	S5	f	High	0.82
Frac N vs. time	S5	f	Low	0.72
Frac N vs. time	S5	f	Medium	0.71
Mass vs. time	S6	a	High	0.79
Mass vs. time	S6	a	Low	0.93
Mass vs. time	S6	a	Medium	0.84
Mass vs. time	S6	b	High	0.72
Mass vs. time	S6	b	Low	0.70
Mass vs. time	S6	b	Medium	0.80
Mass vs. time	S6	c	High	0.87
Mass vs. time	S6	c	Low	0.81
Mass vs. time	S6	c	Medium	0.85
Mass vs. time	S8	a Acer LEAF	High	0.80
Mass vs. time	S8	a Acer LEAF	Low	0.31
LMF vs. time	S8	a Acer LMF	High	0.58
LMF vs. time	S8	a Acer LMF	Low	0.71

Relationship	Figure	Panel	Line	R^2
RMF vs. time	S8	a Acer RMF	High	0.58
RMF vs. time	S8	a Acer RMF	Low	0.71
Mass vs. time	S8	a Acer ROOT	High	0.75
Mass vs. time	S8	a Acer ROOT	Low	0.65
Mass vs. time	S8	a Acer STEM	High	0.86
Mass vs. time	S8	a Acer STEM	Low	0.56
Mass vs. time	S8	a Betula LEAF	High	0.58
LMF vs. time	S8	a Betula LMF	High	0.43
RMF vs. time	S8	a Betula RMF	High	0.43
Mass vs. time	S8	a Betula ROOT	High	0.59
Mass vs. time	S8	a Betula STEM	High	0.75
Mass vs. time	S8	a Liquidambar LEAF	High	0.93
Mass vs. time	S8	a Liquidambar LEAF	Low	0.84
LMF vs. time	S8	a Liquidambar LMF	High	0.10
LMF vs. time	S8	a Liquidambar LMF	Low	0.64
RMF vs. time	S8	a Liquidambar RMF	High	0.10
RMF vs. time	S8	a Liquidambar RMF	Low	0.64
Mass vs. time	S8	a Liquidambar ROOT	High	0.77
Mass vs. time	S8	a Liquidambar ROOT	Low	0.79
Mass vs. time	S8	a Liquidambar STEM	High	0.92
Mass vs. time	S8	a Liquidambar STEM	Low	0.81
Mass vs. time	S8	a Poa. LEAF	High	0.83
Mass vs. time	S8	a Poa. LEAF	Low	0.35
LMF vs. time	S8	a Poa. LMF	High	0.88
LMF vs. time	S8	a Poa. LMF	Low	0.22
RMF vs. time	S8	a Poa. RMF	High	0.88
RMF vs. time	S8	a Poa. RMF	Low	0.22
Mass vs. time	S8	a Poa. ROOT	High	0.77
Mass vs. time	S8	a Poa. ROOT	Low	0.46
Mass vs. time	S8	a Poa. STEM	High	NA
Mass vs. time	S8	a Poa. STEM	Low	NA
Mass vs. time	S8	a Robinia LEAF	High	0.84
LMF vs. time	S8	a Robinia LMF	High	0.29
RMF vs. time	S8	a Robinia RMF	High	0.29
Mass vs. time	S8	a Robinia ROOT	High	0.58
Mass vs. time	S8	a Robinia STEM	High	0.90
Mass vs. time	S8	a Schiz. LEAF	High	0.77
Mass vs. time	S8	a Schiz. LEAF	Low	0.71
LMF vs. time	S8	a Schiz. LMF	High	0.17

Relationship	Figure	Panel	Line	R^2
LMF vs. time	S8	a Schiz. LMF	Low	0.11
RMF vs. time	S8	a Schiz. RMF	High	0.17
RMF vs. time	S8	a Schiz. RMF	Low	0.11
Mass vs. time	S8	a Schiz. ROOT	High	0.82
Mass vs. time	S8	a Schiz. ROOT	Low	0.62
Mass vs. time	S8	a Schiz. STEM	High	NA
Mass vs. time	S8	a Schiz. STEM	Low	NA
Mass vs. time	S8	a Trifolium LEAF	High	0.79
LMF vs. time	S8	a Trifolium LMF	High	0.61
RMF vs. time	S8	a Trifolium RMF	High	0.61
Mass vs. time	S8	a Trifolium ROOT	High	0.72
Mass vs. time	S8	a Trifolium STEM	High	0.62
Mass vs. time	S8	b P.abies LEAF	High	0.98
Mass vs. time	S8	b P.abies LEAF	Low	0.79
LMF vs. time	S8	b P.abies LMF	High	0.48
LMF vs. time	S8	b P.abies LMF	Low	0.66
RMF vs. time	S8	b P.abies RMF	High	0.48
RMF vs. time	S8	b P.abies RMF	Low	0.66
Mass vs. time	S8	b P.abies ROOT	High	0.86
Mass vs. time	S8	b P.abies ROOT	Low	0.90
Mass vs. time	S8	b P.abies STEM	High	0.93
Mass vs. time	S8	b P.abies STEM	Low	0.61
Mass vs. time	S8	b P.banks LEAF	High	0.91
Mass vs. time	S8	b P.banks LEAF	Low	0.73
LMF vs. time	S8	b P.banks LMF	High	0.84
LMF vs. time	S8	b P.banks LMF	Low	0.78
RMF vs. time	S8	b P.banks RMF	High	0.84
RMF vs. time	S8	b P.banks RMF	Low	0.78
Mass vs. time	S8	b P.banks ROOT	High	0.86
Mass vs. time	S8	b P.banks ROOT	Low	0.89
Mass vs. time	S8	b P.banks STEM	High	0.87
Mass vs. time	S8	b P.banks STEM	Low	0.69
Mass vs. time	S8	b P.glauca LEAF	High	0.83
Mass vs. time	S8	b P.glauca LEAF	Low	0.67
LMF vs. time	S8	b P.glauca LMF	High	0.65
LMF vs. time	S8	b P.glauca LMF	Low	0.45
RMF vs. time	S8	b P.glauca RMF	High	0.65
RMF vs. time	S8	b P.glauca RMF	Low	0.45
Mass vs. time	S8	b P.glauca ROOT	High	0.93

Relationship	Figure	Panel	Line	R^2
Mass vs. time	S8	b P.glauca ROOT	Low	0.64
Mass vs. time	S8	b P.glauca STEM	High	0.85
Mass vs. time	S8	b P.glauca STEM	Low	0.75
Mass vs. time	S8	b P.resinosa LEAF	High	0.91
Mass vs. time	S8	b P.resinosa LEAF	Low	0.89
LMF vs. time	S8	b P.resinosa LMF	High	0.85
LMF vs. time	S8	b P.resinosa LMF	Low	0.87
RMF vs. time	S8	b P.resinosa RMF	High	0.86
RMF vs. time	S8	b P.resinosa RMF	Low	0.87
Mass vs. time	S8	b P.resinosa ROOT	High	0.87
Mass vs. time	S8	b P.resinosa ROOT	Low	0.91
Mass vs. time	S8	b P.resinosa STEM	High	0.97
Mass vs. time	S8	b P.resinosa STEM	Low	0.74
Mass vs. time	S8	b P.strobus LEAF	High	0.96
Mass vs. time	S8	b P.strobus LEAF	Low	0.63
LMF vs. time	S8	b P.strobus LMF	High	0.89
LMF vs. time	S8	b P.strobus LMF	Low	0.90
RMF vs. time	S8	b P.strobus RMF	High	0.89
RMF vs. time	S8	b P.strobus RMF	Low	0.90
Mass vs. time	S8	b P.strobus ROOT	High	0.98
Mass vs. time	S8	b P.strobus ROOT	Low	0.84
Mass vs. time	S8	b P.strobus STEM	High	0.92
Mass vs. time	S8	b P.strobus STEM	Low	0.64
Mass vs. time	S8	b P.sylvestris LEAF	High	0.97
Mass vs. time	S8	b P.sylvestris LEAF	Low	0.85
LMF vs. time	S8	b P.sylvestris LMF	High	0.91
LMF vs. time	S8	b P.sylvestris LMF	Low	0.86
RMF vs. time	S8	b P.sylvestris RMF	High	0.91
RMF vs. time	S8	b P.sylvestris RMF	Low	0.86
Mass vs. time	S8	b P.sylvestris ROOT	High	0.98
Mass vs. time	S8	b P.sylvestris ROOT	Low	0.91
Mass vs. time	S8	b P.sylvestris STEM	High	0.94
Mass vs. time	S8	b P.sylvestris STEM	Low	0.82
Mass vs. time	S8	b P.taeda LEAF	High	0.89
Mass vs. time	S8	b P.taeda LEAF	Low	0.89
LMF vs. time	S8	b P.taeda LMF	High	0.85
LMF vs. time	S8	b P.taeda LMF	Low	0.65
RMF vs. time	S8	b P.taeda RMF	High	0.85
RMF vs. time	S8	b P.taeda RMF	Low	0.65

Relationship	Figure	Panel	Line	R^2
Mass vs. time	S8	b P.taeda ROOT	High	0.82
Mass vs. time	S8	b P.taeda ROOT	Low	0.87
Mass vs. time	S8	b P.taeda STEM	High	0.98
Mass vs. time	S8	b P.taeda STEM	Low	0.76
[N] vs. time	S9	a Acer LEAFnc	High	0.22
[N] vs. time	S9	a Acer LEAFnc	Low	0.26
[N] vs. time	S9	a Acer ROOTnc	High	0.56
[N] vs. time	S9	a Acer ROOTnc	Low	0.30
[N] vs. time	S9	a Acer STEMnc	High	0.26
[N] vs. time	S9	a Acer STEMnc	Low	0.36
[N] vs. time	S9	a Betula LEAFnc	High	0.47
[N] vs. time	S9	a Betula ROOTnc	High	0.54
[N] vs. time	S9	a Betula STEMnc	High	0.44
[N] vs. time	S9	a Liquidambar LEAFnc	High	0.57
[N] vs. time	S9	a Liquidambar LEAFnc	Low	0.73
[N] vs. time	S9	a Liquidambar ROOTnc	High	0.46
[N] vs. time	S9	a Liquidambar ROOTnc	Low	0.23
[N] vs. time	S9	a Liquidambar STEMnc	High	0.51
[N] vs. time	S9	a Liquidambar STEMnc	Low	0.46
[N] vs. time	S9	a Poa. LEAFnc	High	0.33
[N] vs. time	S9	a Poa. LEAFnc	Low	0.33
[N] vs. time	S9	a Poa. ROOTnc	High	0.40
[N] vs. time	S9	a Poa. ROOTnc	Low	0.34
[N] vs. time	S9	a Poa. STEMnc	High	NA
[N] vs. time	S9	a Poa. STEMnc	Low	NA
[N] vs. time	S9	a Robinia LEAFnc	High	0.82
[N] vs. time	S9	a Robinia ROOTnc	High	0.39
[N] vs. time	S9	a Robinia STEMnc	High	0.32
[N] vs. time	S9	a Schiz. LEAFnc	High	0.56
[N] vs. time	S9	a Schiz. LEAFnc	Low	0.25
[N] vs. time	S9	a Schiz. ROOTnc	High	0.43
[N] vs. time	S9	a Schiz. ROOTnc	Low	0.30
[N] vs. time	S9	a Schiz. STEMnc	High	NA
[N] vs. time	S9	a Schiz. STEMnc	Low	NA
[N] vs. time	S9	a Trifolium LEAFnc	High	0.51
[N] vs. time	S9	a Trifolium ROOTnc	High	0.77

Relationship	Figure	Panel	Line	R^2
[N] vs. time	S9	a Trifolium STEMnc	High	0.23
[N] vs. time	S9	b P.abies LEAFnc	High	0.65
[N] vs. time	S9	b P.abies LEAFnc	Low	0.50
[N] vs. time	S9	b P.abies ROOTnc	High	0.74
[N] vs. time	S9	b P.abies ROOTnc	Low	0.61
[N] vs. time	S9	b P.abies STEMnc	High	0.76
[N] vs. time	S9	b P.abies STEMnc	Low	0.30
[N] vs. time	S9	b P.banks LEAFnc	High	0.73
[N] vs. time	S9	b P.banks LEAFnc	Low	0.51
[N] vs. time	S9	b P.banks ROOTnc	High	0.87
[N] vs. time	S9	b P.banks ROOTnc	Low	0.57
[N] vs. time	S9	b P.banks STEMnc	High	0.49
[N] vs. time	S9	b P.banks STEMnc	Low	0.23
[N] vs. time	S9	b P.glauca LEAFnc	High	0.89
[N] vs. time	S9	b P.glauca LEAFnc	Low	0.63
[N] vs. time	S9	b P.glauca ROOTnc	High	0.51
[N] vs. time	S9	b P.glauca ROOTnc	Low	0.39
[N] vs. time	S9	b P.glauca STEMnc	High	0.25
[N] vs. time	S9	b P.glauca STEMnc	Low	0.29
[N] vs. time	S9	b P.resinosa LEAFnc	High	0.94
[N] vs. time	S9	b P.resinosa LEAFnc	Low	0.38
[N] vs. time	S9	b P.resinosa ROOTnc	High	0.80
[N] vs. time	S9	b P.resinosa ROOTnc	Low	0.88
[N] vs. time	S9	b P.resinosa STEMnc	High	0.77
[N] vs. time	S9	b P.resinosa STEMnc	Low	0.89
[N] vs. time	S9	b P.strobus LEAFnc	High	0.80
[N] vs. time	S9	b P.strobus LEAFnc	Low	0.73
[N] vs. time	S9	b P.strobus ROOTnc	High	0.78
[N] vs. time	S9	b P.strobus ROOTnc	Low	0.26
[N] vs. time	S9	b P.strobus STEMnc	High	0.83
[N] vs. time	S9	b P.strobus STEMnc	Low	0.75
[N] vs. time	S9	b P.sylvestris LEAFnc	High	0.65
[N] vs. time	S9	b P.sylvestris LEAFnc	Low	0.50
[N] vs. time	S9	b P.sylvestris ROOTnc	High	0.74
[N] vs. time	S9	b P.sylvestris ROOTnc	Low	0.61
[N] vs. time	S9	b P.sylvestris STEMnc	High	0.76
[N] vs. time	S9	b P.sylvestris STEMnc	Low	0.30
[N] vs. time	S9	b P.taeda LEAFnc	High	0.76
[N] vs. time	S9	b P.taeda LEAFnc	Low	0.81

Relationship	Figure	Panel	Line	R^2
[N] vs. time	S9	b P.taeda ROOTnc	High	0.51
[N] vs. time	S9	b P.taeda ROOTnc	Low	0.89
[N] vs. time	S9	b P.taeda STEMnc	High	0.25
[N] vs. time	S9	b P.taeda STEMnc	Low	0.27
Total N vs. time	S10	a Acer	High	0.86
Total N vs. time	S10	a Acer	Low	0.68
Total N vs. time	S10	a Betula	High	0.50
Total N vs. time	S10	a Liquidambar	High	0.90
Total N vs. time	S10	a Liquidambar	Low	0.70
Total N vs. time	S10	a Poa.	High	0.85
Total N vs. time	S10	a Poa.	Low	0.47
Total N vs. time	S10	a Robinia	High	0.58
Total N vs. time	S10	a Schiz.	High	0.71
Total N vs. time	S10	a Schiz.	Low	0.90
Total N vs. time	S10	a Trifolium	High	0.87
Total N vs. time	S10	b P.abies	High	0.94
Total N vs. time	S10	b P.abies	Low	0.78
Total N vs. time	S10	b P.banks	High	0.82
Total N vs. time	S10	b P.banks	Low	0.64
Total N vs. time	S10	b P.glauca	High	0.74
Total N vs. time	S10	b P.glauca	Low	0.78
Total N vs. time	S10	b P.resinosa	High	0.85
Total N vs. time	S10	b P.resinosa	Low	0.86
Total N vs. time	S10	b P.strobus	High	0.94
Total N vs. time	S10	b P.strobus	Low	0.68
Total N vs. time	S10	b P.sylvestris	High	0.93
Total N vs. time	S10	b P.sylvestris	Low	0.46
Total N vs. time	S10	b P.taeda	High	0.86
Total N vs. time	S10	b P.taeda	Low	0.76
Mass vs. time	S12	a S1, P2	Total	0.97
Mass vs. time	S12	a S1, P2	Schiz	1.00
Mass vs. time	S12	a S1, P2	Poa	1.00
Mass vs. time	S12	a S3, P6	Total	0.99
Mass vs. time	S12	a S3, P6	Schiz	1.00
Mass vs. time	S12	a S3, P6	Poa	1.00
Mass vs. time	S12	a S2, P1	Total	0.98
Mass vs. time	S12	a S2, P1	Schiz	1.00
Mass vs. time	S12	a S2, P1	Poa	1.00
Mass vs. time	S12	a S6, P3	Total	0.99

Relationship	Figure	Panel	Line	R^2
Mass vs. time	S12	a S6, P3	Schiz	1.00
Mass vs. time	S12	a S6, P3	Poa	1.00
Mass vs. time	S12	b S1, P2	Total	0.95
Mass vs. time	S12	b S1, P2	Schiz	0.60
Mass vs. time	S12	b S1, P2	Poa	0.92
Mass vs. time	S12	b S3, P6	Total	0.98
Mass vs. time	S12	b S3, P6	Schiz	0.73
Mass vs. time	S12	b S3, P6	Poa	0.97
Mass vs. time	S12	b S2, P1	Total	0.97
Mass vs. time	S12	b S2, P1	Schiz	0.55
Mass vs. time	S12	b S2, P1	Poa	0.89
Mass vs. time	S12	b S6, P3	Total	0.98
Mass vs. time	S12	b S6, P3	Schiz	0.86
Mass vs. time	S12	b S6, P3	Poa	0.97
RMF vs. time	S12	c S1, P2	Total	0.48
RMF vs. time	S12	c S1, P2	Schiz	1.00
RMF vs. time	S12	c S1, P2	Poa	1.00
RMF vs. time	S12	c S3, P6	Total	0.65
RMF vs. time	S12	c S3, P6	Schiz	1.00
RMF vs. time	S12	c S3, P6	Poa	1.00
RMF vs. time	S12	c S2, P1	Total	0.53
RMF vs. time	S12	c S2, P1	Schiz	1.00
RMF vs. time	S12	c S2, P1	Poa	1.00
RMF vs. time	S12	c S6, P3	Total	0.35
RMF vs. time	S12	c S6, P3	Schiz	1.00
RMF vs. time	S12	c S6, P3	Poa	1.00
Mass vs. time	S12	d S1, P2	Total	0.91
Mass vs. time	S12	d S1, P2	Schiz	1.00
Mass vs. time	S12	d S1, P2	Poa	1.00
Mass vs. time	S12	d S3, P6	Total	0.98
Mass vs. time	S12	d S3, P6	Schiz	1.00
Mass vs. time	S12	d S3, P6	Poa	1.00
Mass vs. time	S12	d S2, P1	Total	0.95
Mass vs. time	S12	d S2, P1	Schiz	1.00
Mass vs. time	S12	d S2, P1	Poa	1.00
Mass vs. time	S12	d S6, P3	Total	0.96
Mass vs. time	S12	d S6, P3	Schiz	1.00
Mass vs. time	S12	d S6, P3	Poa	1.00
[N] vs. time	S13	a S1, P2	Schiz	0.85

Relationship	Figure	Panel	Line	R^2
[N] vs. time	S13	a S1, P2	Poa	0.97
[N] vs. time	S13	a S3, P6	Schiz	0.51
[N] vs. time	S13	a S3, P6	Poa	0.98
[N] vs. time	S13	a S2, P1	Schiz	0.84
[N] vs. time	S13	a S2, P1	Poa	0.97
[N] vs. time	S13	a S6, P3	Schiz	0.69
[N] vs. time	S13	a S6, P3	Poa	0.95
[N] vs. time	S13	b S1, P2	Schiz	0.69
[N] vs. time	S13	b S1, P2	Poa	0.47
[N] vs. time	S13	b S3, P6	Schiz	0.54
[N] vs. time	S13	b S3, P6	Poa	0.88
[N] vs. time	S13	b S2, P1	Schiz	0.70
[N] vs. time	S13	b S2, P1	Poa	0.60
[N] vs. time	S13	b S6, P3	Schiz	0.39
[N] vs. time	S13	b S6, P3	Poa	0.27
Total N vs. time	S14	S1, P2	Total	0.95
Total N vs. time	S14	S1, P2	Schiz	0.59
Total N vs. time	S14	S1, P2	Poa	0.87
Total N vs. time	S14	S3, P6	Total	0.98
Total N vs. time	S14	S3, P6	Schiz	0.55
Total N vs. time	S14	S3, P6	Poa	0.97
Total N vs. time	S14	S2, P1	Total	0.98
Total N vs. time	S14	S2, P1	Schiz	0.45
Total N vs. time	S14	S2, P1	Poa	0.85
Total N vs. time	S14	S6, P3	Total	0.98
Total N vs. time	S14	S6, P3	Schiz	0.78
Total N vs. time	S14	S6, P3	Poa	0.94
Total N vs. time	S16	a	High	0.70
Total N vs. time	S16	a	Low	0.75
Total N vs. time	S16	b	Soil	0.90
Total N vs. time	S16	c	High	0.89
Total N vs. time	S16	c	Low	0.95
Total N vs. time	S16	d	Soil	0.86
Mass vs. time	S16	e	High	0.70
Mass vs. time	S16	e	Low	0.68
Mass vs. time	S16	f	Soil	0.72
Mass vs. time	S16	g	High	0.84
Mass vs. time	S16	g	Low	0.92
Mass vs. time	S16	h	Soil	0.78

1061